Journal of Medicinal Chemistry

Article

Amino acids bearing aromatic or heteroaromatic substituents as a new class of ligands for the lysosomal sialic acid transporter sialin (SLC17A5)

Lilian Dubois, Nicolas Pietrancosta, Alexandre Cabaye, Isabelle Fanget, Cécile Debacker, Pierre-André Gilormini, Patrick M Dansette, Julien Dairou, Christophe Biot, Roseline Froissart, Anne Goupil-Lamy, Hugues-Olivier Bertrand, Francine Clemy Acher, Isabelle McCort-Tranchepain, Bruno Gasnier, and Christine Anne

J. Med. Chem., **Just Accepted Manuscript** • DOI: 10.1021/acs.jmedchem.9b02119 • Publication Date (Web): 01 Jul 2020

Amino acids bearing aromatic or heteroaromatic substituents as a new class of ligands for the lysosomal sialic acid transporter sialin (SLC17A5)

Lilian Dubois,[1] Nicolas Pietrancosta,[2,3] Alexandre Cabaye,[1,4] Isabelle Fanget,[5] Cécile Debacker,[5] Pierre-André Gilormini,[6‡] Patrick Dansette,[1] Julien Dairou,[1] Christophe Biot,[6] Roseline Froissart,[7] Anne Goupil-Lamy,[4] Hugues-Olivier Bertrand,[4] Francine Acher,[1] Isabelle McCort-Tranchepain,[1] Bruno Gasnier,[5*] and Christine Anne [5*]*

1 Université de Paris, Laboratoire de Chimie et Biochimie Pharmacologiques et Toxicologiques, CNRS, UMR 8601, F-75006 Paris, France

2 Sorbonne Université, École Normale Supérieure, PSL University, CNRS, Laboratoire des Biomolécules, LBM, F-75005 Paris, France.

3 Sorbonne Université, INSERM, CNRS, Neurosciences Paris Seine - Institut de Biologie Paris Seine (NPS - IBPS), F-75005, Paris, France.

4 BIOVIA, Dassault Systèmes, F-78140 Velizy-Villacoublay, France

5 Université de Paris, SPPIN - Saints-Pères Paris Institute for the Neurosciences, CNRS, F-75006 Paris, France

6 Université de Lille, CNRS, UMR 8576, UGSF, Unité de Glycobiologie et Fonctionnelle, F-59650 Lille, France

7 Service de Biochimie et Biologie Moléculaire Grand Est, Centre de Biologie et de Pathologie Est, Hospices Civils de Lyon, F-69677 Bron, France

ABSTRACT: Sialin is a lysosomal sialic acid transporter defective in Salla disease, a rare inherited leukodystrophy. It also enables metabolic incorporation of exogenous sialic acids, leading to autoantibodies against *N*-glycolylneuraminic acid in humans. Here we identified a novel class of human sialin ligands by virtual screening and structure-activity relationship studies. The ligand scaffold is characterized by an amino acid backbone with a free carboxylate, an *N*-linked aromatic or heteroaromatic substituent and a hydrophobic side chain. The most potent compound, **45** (LSP12-3129), inhibited *N*-acetylneuraminic acid **1** (Neu5Ac) transport in a non-competitive manner with $IC_{50} \approx 2.5$ μM, a value 400-fold lower than the K_M for Neu5Ac. In vitro and molecular docking studies attributed the non-competitive character to selective inhibitor binding to the Neu5Ac site in cytosol-facing conformation. Moreover, compound **45** rescued the trafficking defect of the pathogenic mutant (R39C) causing Salla disease. This new class of cell-permeant inhibitors provide tools to investigate the physiological roles of sialin and to help develop pharmacological chaperones for Salla disease.

Introduction

SLC17 transporters, a subgroup from the major facilitator superfamily (MFS) of secondary active transporters, are involved in the excretion of urate and other organic anions in the kidney, the uptake of anionic neurotransmitters (glutamate, ATP) into synaptic vesicles, and the export of sialic acids and acidic hexoses from lysosomes for reuse in metabolism.[1–7] The latter function is ensured by sialin, a H^+/sialic acid symporter encoded by the SLC17A5 gene.[5–7] Owing to its H^+ coupling and the steep pH gradient (~ 2.5 units) across the lysosomal membrane, sialin actively exports sialic acids from the lysosomal lumen, thus contributing with de novo biosynthesis to their cytosolic availability. This in turn impacts the sialylation of cell surface glycoconjugates and their role in cell-cell, cell-extracellular matrix and cell-pathogen interactions. Sialin has also been implicated in the uptake of nitrate at the plasma membrane[8] and the uptake of aspartate, glutamate and *N*-acetyl-aspartyl-glutamate into synaptic vesicles.[9,10]

In addition to its role in recycling endogenous sialic acids, lysosomal export by sialin enables the metabolic incorporation of exogenous sialic acids internalized by fluid phase endocytosis,[11] thus circumventing the absence of sialic acid transporter at the plasma membrane. This endocytic route impacts human health by incorporating dietary-derived *N*-glycolylneuraminic acid (Neu5Gc) into glycoconjugates. Owing to a mutation in the cytidine monophosphate-Neu5Ac hydroxylase (CMAH) gene, humans do not synthesize this sialic acid which is abundant in other species.[12] Neu5Gc is thus incorporated into human cell glycans, inducing the production of anti-Neu5GC autoantibodies associated with chronic inflammation, cancer and atherosclerosis.[13,14] This endocytic route is also exploited in glycoengineering approaches to alter cell surface glycans with synthetic sialic acid derivatives and thereby: modulate immune responses; inhibit pathogen binding; target toxins to tumors; or track cells in vivo after transplantation.[15,16]

The essential role of sialin in sialic acid homeostasis is also highlighted by its inactivation in two autosomal recessive genetic diseases, Salla disease and Infantile free Sialic acid Storage Disease (ISSD).[5,17,18] Both diseases are associated with defective lysosomal export of sialic acids,[6,7,19] leading to their accumulation in diverse tissues and their excretion in urine. However, they strongly differ in clinical course and severity. While ISSD affects multiple organs from birth, causing death within a few months or years, Salla disease selectively affects the white matter of the brain in a progressive manner.[17,20,21] Salla patients show hypotonia, ataxia, nystagmus and delayed motor development during the first year. Psychomotor milestones, including speech, progressively worsens during infancy and childhood, leading to severe motor and cognitive deficits in adulthood. Magnetic resonance imaging shows nonspecific brain hypomyelination with a thinning of the corpus callosum.[22] Current treatment is supportive.

The pathophysiology of Salla disease remains poorly understood. Sialin-defective mice studies have shown that brain hypomyelination results from defective maturation of oligodendrocytes[23,24]. However, the link between this defect and defective lysosomal sialic acid export, or other transport activities of sialin[9] (but see ref.[25]), is unclear. Decreased downregulation of the polysialylated Neural Cell Adhesion Molecule (PSA-NCAM), which could delay oligodendrocyte/axon contacts, may be involved.[23] However, this decrease is limited, indicating that other mechanisms, such as impaired ganglioside metabolism,[26] should contribute to the myelination defect.

On the other hand, genotype-phenotype relationship studies have shown a clear correlation between the level of Neu5Ac transport and the clinical severity induced by SLC17A5 mutations. Salla disease is almost exclusively associated with one missense mutation, R39C, in homozygous or compound-heterozygous state which partially impairs lysosomal targeting of sialin[6,27] and which decreases its transport activity to ~20% of wild-type level[6,7] whereas ISSD-associated

mutations abolish either the expression or the transport activity of sialin.[6,7,18] The association of Salla disease with residual sialic acid transport has been confirmed in a rare case of patient with a homozygous K136E mutation,[28] which also partially preserves sialic acid transport and lysosomal localization.[6,7] The trafficking defect may result from destabilization of the R39C and K136E mutants, and their retention by the protein quality control system. This feature along with the residual transport activity and the overwhelming predominance of the R39C mutation suggest pharmacological chaperone therapy as a promising option to treat Salla disease.

In contrast with other SLC17 transporters such as VGLUT[29–31] and VNUT[32] proteins, we lack pharmacological tools to study the cellular and physiological roles of sialin or to help rescue the R39C mutant causing Salla disease. In a previous study,[33] we characterized the interaction of human sialin with synthetic sialic acids and identified one compound with IC50 ≈ 40 μM, a value 25-fold lower than the K_M for Neu5Ac. We also built a cytosol-facing homology model of human sialin based on a distantly homologous MFS crystallographic structure, the glycerol-3-phosphate transporter (GlpT) from E. coli.[34] After validating the sialic acid-binding site of this model by site-directed mutagenesis, virtual screening against the ZINC database and Neu5Ac transport studies led us to identify the artificial tripeptide FR139317 as a new sialin ligand unrelated to sialic acids.[33] In this study, we disclose other virtual hits from this screen and identify a novel scaffold of sialin ligand well suited for chemical modifications. After optimization, the new ligands obtained inhibit sialin with a μM affinity in a non-competitive manner and one of them could partially rescue the trafficking defect of the pathogenic R39C mutant.

Results

Screening and Scaffold Selection. Our previous virtual screening of a GlpT-based homology model of human sialin against a subset of the ZINC database[35] (~12,000 compounds) identified the endothelin-A receptor antagonist FR139317 **2** and eight other molecules[33] (Figure 1A) as candidate sialin ligands. Transport studies confirmed **2** as a competitive inhibitor of *N*-acetylneuraminic acid **1** (Neu5Ac) transport by human sialin with a K_i of 20 μM, a value ~50-fold lower than the K_M for Neu5Ac.[33] We thus tested the other compounds using the same transport assay, which is based on a sorting mutant (L22G/L23G) redirected to the plasma membrane.[6] In this approach, the poorly tractable lysosomal export is replaced by a whole-cell [^{3}H]Neu5Ac uptake in acidic extracellular buffer to mimic the lysosomal lumen and facilitate transport measurements (Figure 1B). This technique provides higher signal-to-noise ratios than lysosomal assays, with highly similar Neu5Ac transport properties.[6]

Among the novel virtual hits, four compounds inhibited Neu5Ac uptake and three of them, Fmoc-Lys(Cbz)-OH **3**, Fmoc-D-Phe(*p*CH_2NHBoc)-OH **4** and calcein **5** were more efficient inhibitors than Neu5Ac (Figure 1C). Interestingly, **3** and **4** are both amino acid derivatives with common features: the α amine is protected by the same hydrophobic carbamate, (Fluoren-9-yl)methoxycarbonyl (Fmoc); the carboxylic acid is free; and a 4 to 6-carbon side chain bears a distal amine protected by a benzyloxycarbonyl (Cbz) or *tert*-butoxycarbonyl (Boc) group.

A

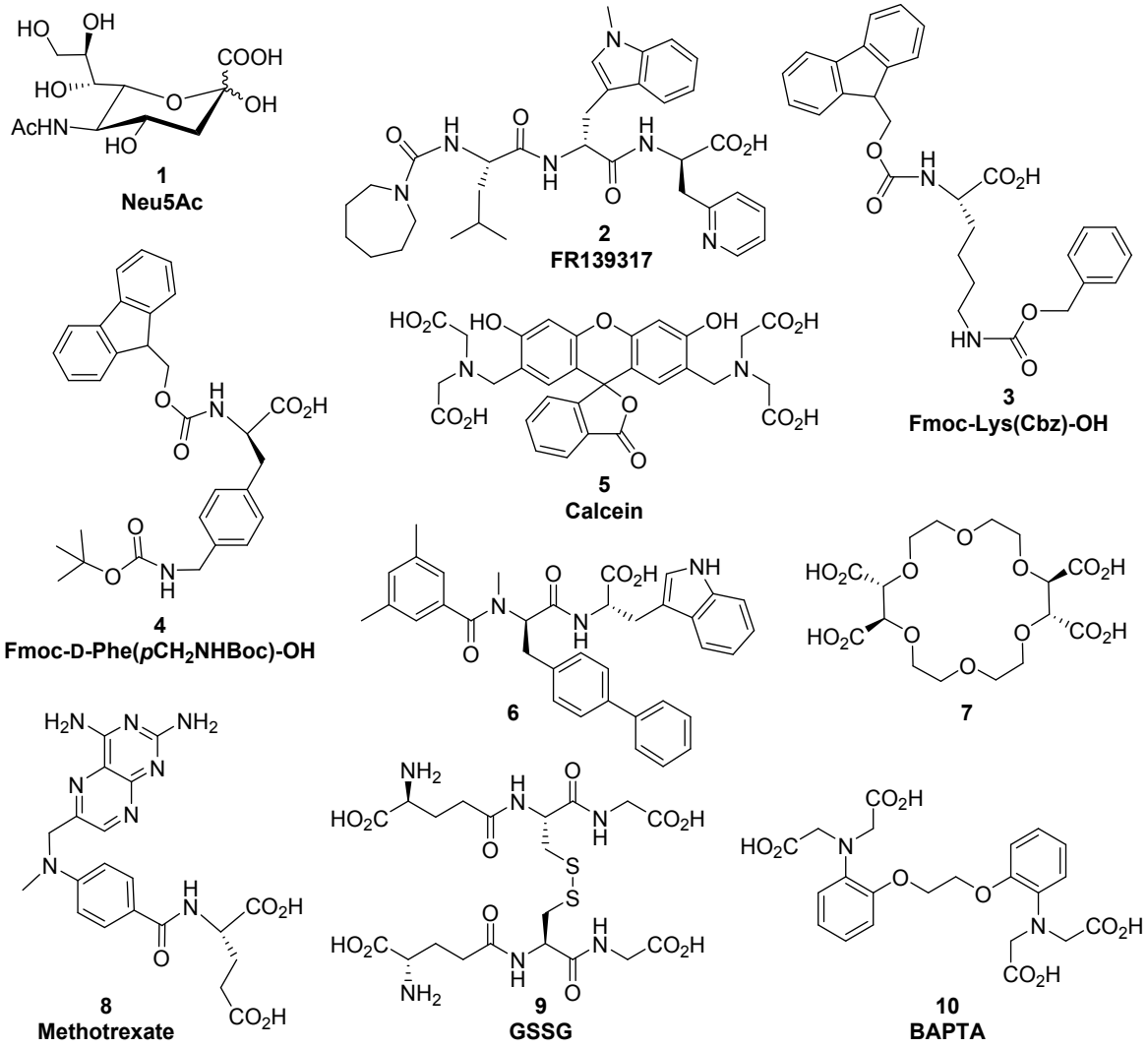
1
Neu5Ac
2
FR139317
3
Fmoc-Lys(Cbz)-OH
4
Fmoc-D-Phe(pCH2NHBoc)-OH
5
Calcein
6
7
8
Methotrexate
9
GSSG
10
BAPTA

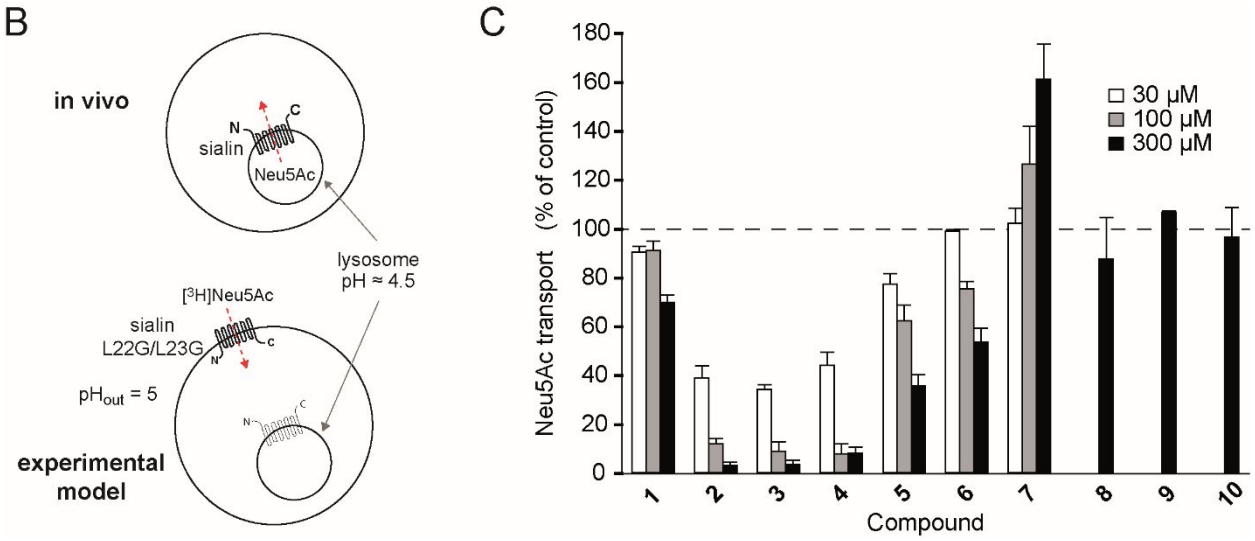
B
in vivo
sialin
Neu5Ac
lysosome
pH ≈ 4.5
[3H]Neu5Ac
sialin
L22G/L23G
pHout = 5
experimental
model
C
Neu5Ac transport (% of control)
30 μM
100 μM
300 μM
Compound

Figure 1. Identification of novel sialin inhibitors (A) Structures (**2** to **10**) of the best hits from a previous virtual screening.[33] (B) Whole-cell assay of human sialin. Mutation of its lysosomal sorting motif redirects sialin to the plasma membrane to facilitate transport measurements. (C) Human sialin was assayed for [^{3}H]Neu5Ac uptake at pH 5.0 in the absence (control) or presence of these compounds (means ± SEM of 2 to 4 independent experiments).

These similarities suggested a novel scaffold recognized by sialin. To test this hypothesis, we evaluated a series of 14 *N*-Fmoc amino acids **11**–**24** in our transport assay (see structures in Supplementary Information, pp. S3-S4). *N*-Fmoc amino acids **11**, **12**, **16**, **22** and **24** were prepared according to classical method (see Supporting information), whereas compounds **13**–**15**, **17**–**21** and **23** were commercially available. Interestingly, 10 out of 14 compounds inhibited Neu5Ac uptake with an efficiency greater than, or similar to, compounds **3** and **4** (Figure 2), thus confirming the existence of a novel scaffold characterized by an *N*-Fmoc group, a free carboxylate, and a hydrophobic side chain. The lower activity of compounds **22**-**24** may result from the presence of a bulkier side chain (compare Fmoc-Lys(Fmoc)-OH **24** with **3**) or from a constrained ring structure of the side chain in Fmoc-Pro-OH **23**. All tested amino acids, except Fmoc-DL-Leu-OH **12**, belonged to the L-series. Comparison of the racemic **12** and L- **13** forms of Fmoc-Leu-OH suggests that the α carbon configuration is not critical to bind sialin (Figure 2).

To characterize further this sialin ligand scaffold, we examined the influence of the proximal amine substitution. The 9-fluorenylmethoxycarbonyl group of compound **3** was thus replaced by a coumarinyl; quinolinyl; xanthenyl; or anthracenyl group linked to the α amine by an amide or carbamate bond. In another set of compounds, we examined the influence of substituents attached to the side chain. For this purpose, we first introduced a 4-methylcarbonylcoumarin instead of Cbz

in compound **3** and then selected compound **16** among those with a good activity to alter the side chain because the sulfanyl group allows alkylation with substituted coumarins in a metabolically stable manner (resistance to cytosolic and lysosomal hydrolases). The synthesis and biological activity of the resulting compounds are described in the next sections.

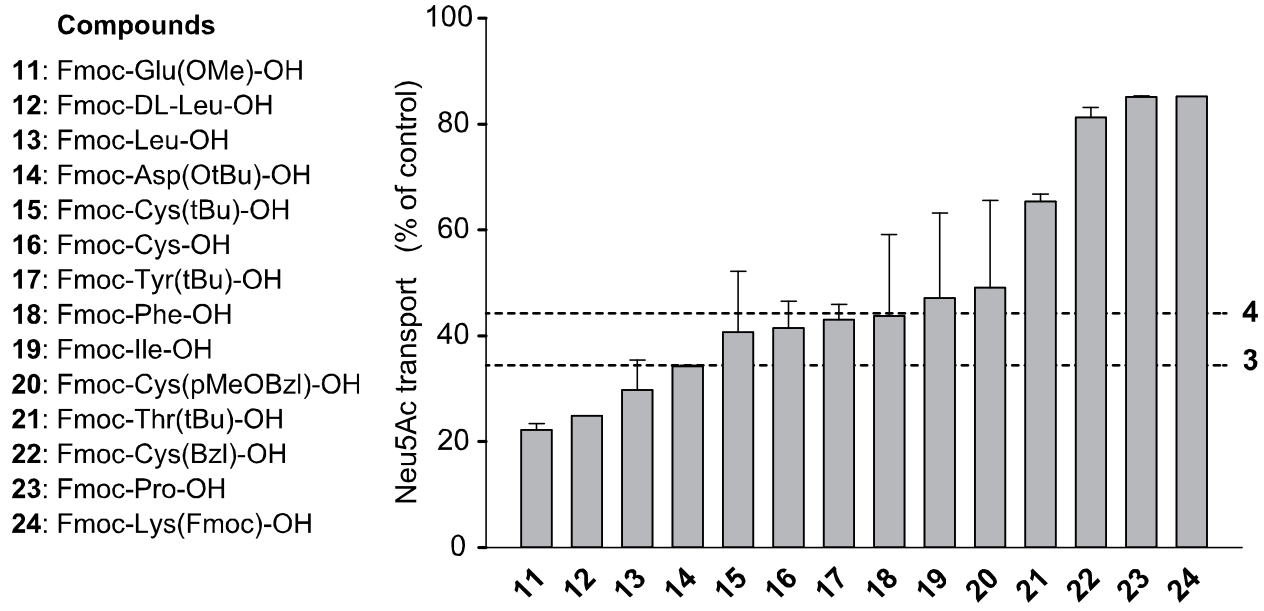

Figure 2. *N*-Fmoc amino acids (30 μM) were tested for inhibition of human sialin as in Figure 1. The dotted lines correspond to the inhibition by compounds **3** and **4**.

Chemistry. All 7-hydroxy 4-substituted coumarins were synthetized via Pechmann condensation in good yields using either Brønsted acid with resorcinol or Lewis acid with an aminophenol derivative (Scheme 1). Compounds **25–28** were prepared according to conventional methods with slight improvements[36–38] (see Supporting information).

Using chlorotriisopropoxytitanium (IV)[39] was more efficient than zinc (II) chloride[40] for the synthesis of 7-(dialkylamino)coumarins **29** and **30.** The xanthenyl derivative **32** was obtained

according to a known procedure[41] as the 3-(3,6-dihydroxy-9*H*-xanthen-9-ylidene)propionic acid tautomer, unambiguously shown by NMR in aprotic solvent (DMSO).

Regioselective protection of the 7-hydroxy-4-hydroxymethyl-coumarin **27** with methoxymethyl chloride before introducing the 9*H*-fluoren-9-yl methyl carbonate in the benzylic position and deprotection of the 7-hydroxyl led to **35**.

Scheme 1. Synthesis of functionalized coumarins[a]

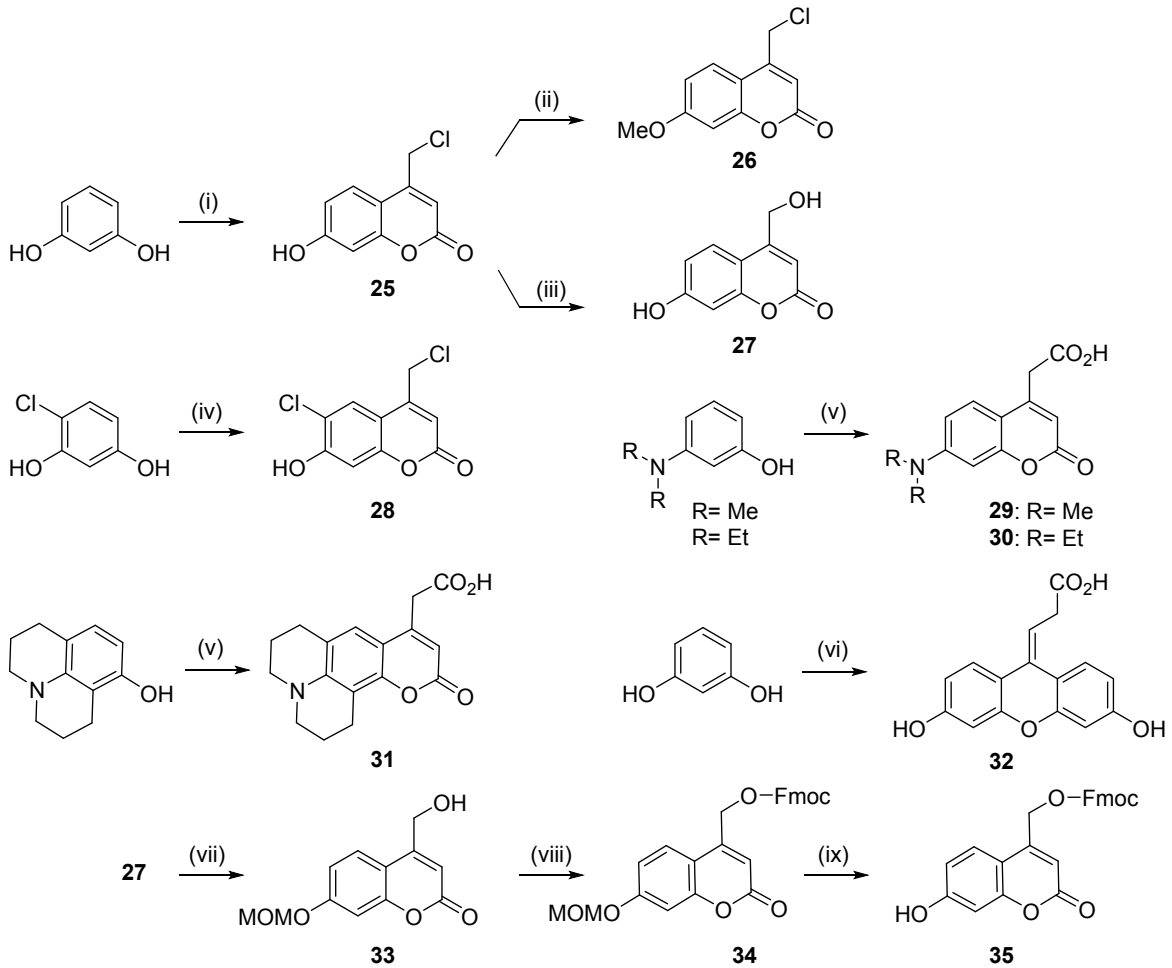

[a]Reagents and conditions: (i) Ethyl-4-chloroacetoacetate, 70% aq H_2SO_4, 0 °C, 1.5 h, 97%; (ii) K_2CO_3, acetone, Me_2SO_4, RT, overnight, 94%; (iii) H_2O, reflux, 48 h, 69%; (iv) Ethyl-4-chloroacetoacetate, CH_3SO_3H RT, 4 h, 97%; (v) (a) $ClTi(OiPr)_3$, dimethyl 3-oxoglutarate, toluene, reflux, overnight; (b) NaOH, MeOH, RT, overnight, 35–66% (two steps); (vi) Succinic anhydride,

70% aq H_2SO_4, 140 °C, 4 h, 92%; (vii) MOM-Cl, DIEA, CH_2Cl_2, 0 °C, 45 min, 71%; (viii) Fmoc-Cl, pyridine, RT, 2 h, 34%; (ix) TFA, CH_2Cl_2, 0 °C then RT, 1.5 h, 83%.

Amide bond formation between the amine of a lysine-OMe derivative and acids **29-32** as well as commercially available 7-hydroxy-4-carboxymethyl-coumarin and 4-carboxyquinolin-2-one were carried out[42] (Scheme 2). Attempts to condense previously activated 7-hydroxy-4-carboxymethyl coumarin as an acid chloride or HOBt ester in presence of EDC with Lys (Cbz)-OMe failed. In contrast, amide bond formation occurred in presence of HBTU, HOBt via uronium salt activation[43,44] with this 4-carboxymethyl-coumarin or with xanthene **32**, leading after saponification of the methyl ester to 36 and 40 in poor yields (19% and 8%, respectively). The condensation of **29**, **30**, 4-carboxyquinolin-2-one and **31** with Lys(Cbz)-OMe performed in the presence of HBTU in CH_2Cl_2 also led to the expected products, generally in better yields (12–50%)[45]. In contrast, under these conditions, the coupling of **29** to the distal amine of lysine **43** was poorly efficient (5%, not optimized). The carbamate analog **44** of **36** was obtained from **27** with carbonyl diimidazole activation.

Scheme 2. Synthesis of *N*-acyl and *N*-carbamate diprotected lysine[a]

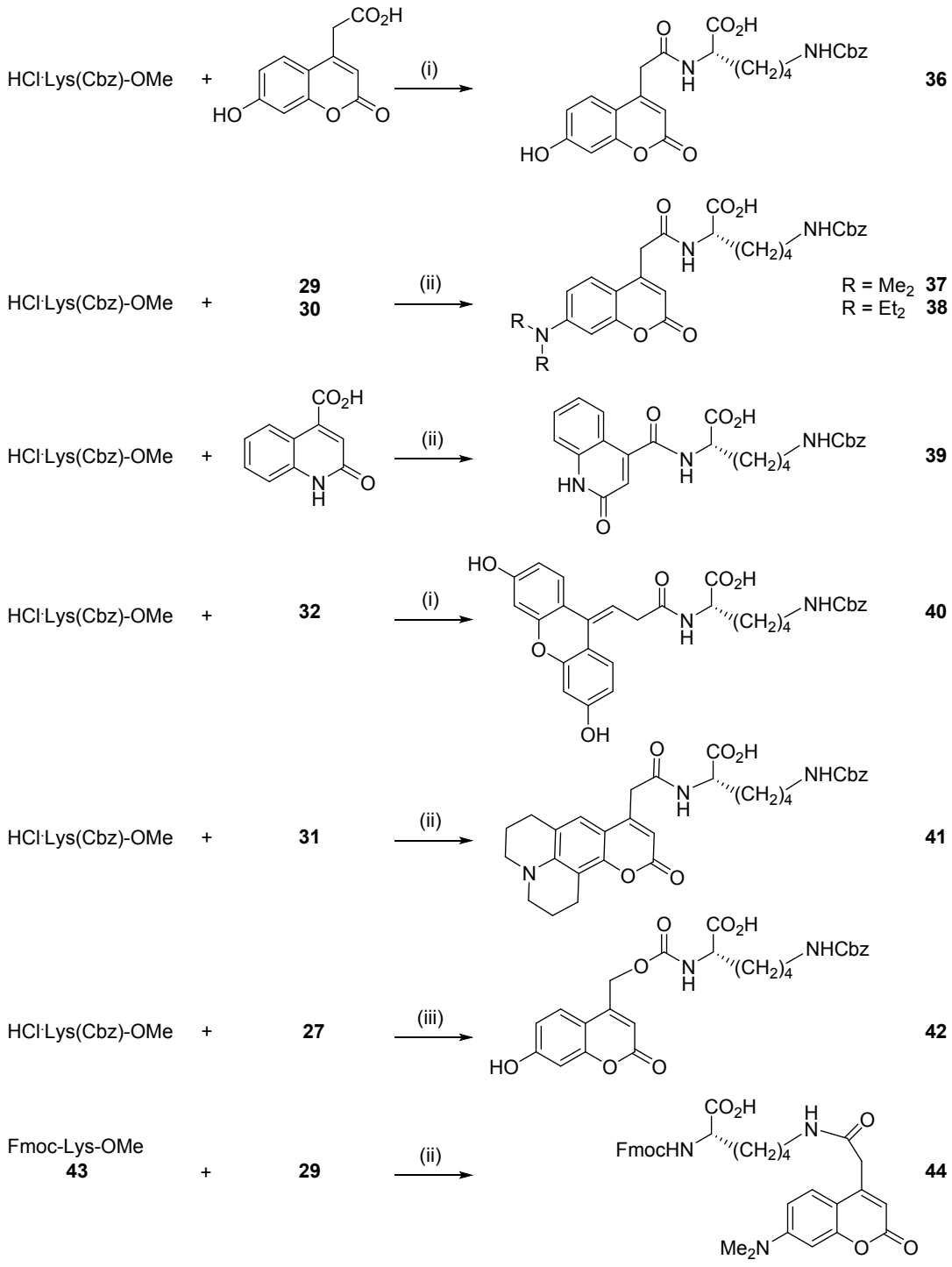

[a]Reagents and conditions: (i) (a) HBTU, HOBt, DMF, DIEA, RT, overnight; (b) aq LiOH, THF, RT, 2 h, 19% for **36**, 8% for **40** (two steps); (ii) (a) HBTU, CH_2Cl_2, DIEA, RT, 2 h; (b) aq LiOH, THF, RT, 2 h, 50% for **37**, 19% for **38,** 43% for **39**, 12% for **41**, 5% for **44** (two steps); (iii) (a) CDI, DMF, DIEA, RT then 80 °C, 1.5 h, 21%; (b) aq LiOH, THF, RT, 2 h 21% (two steps).

Alkylation of Fmoc-Cys-OH by coumarins **25**, **26** and **28** proceeded at room temperature overnight in presence of an excess of base to give compounds **45**–**47** around 30% yields (Scheme 3).

Scheme 3. Synthesis of *S*-alkyl cysteine[a]

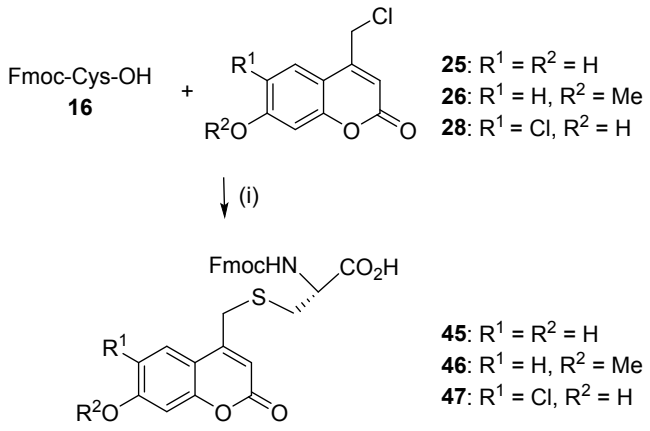

[a]Reagents and conditions: (i) from **25** and **28**; DIEA, THF, RT, 16 h, 35% and 32% respectively; from **26**: Et_3N, DMF, RT, 16 h, 28%.

Structure-Activity Analysis of the Heterocycle-Substituted Amino Acids. Compounds **35**–**42**, and **44** (see structures in Supplementary Information, pp. S3-S4) were tested in our whole-cell assay of sialin at 30 μM (Figure 3) as for the Fmoc-amino acids **11**–**24**. When 9-fluorenylmethyl carbonate is directly linked to the coumarin **27**, the resulting compound **35** does not significantly inhibit sialin, showing that removal of the amino acid backbone and the free carboxylate abolishes binding. Replacing the 9-fluorenylmethyl carbamate linked to the α amine in **3** by diverse heterocycles in compounds **36**–**41** reduced activity, ranging from a moderate loss with the bulky coumarin derivative **41** to virtually no inhibition with the quinolinyl compound **39**. No significant difference was observed among coumarinyl derivatives **36**–**38** bearing different

substituents at the 7-position (hydroxy, dimethyl or diethylamino). Of note, when the amide bond of **36** was converted into a more flexible carbamate bond in **42**, the affinity for sialin increased to a level similar to that of compound **3**.

The influence of substituting the side chain was tested in compounds **44**–**47**. Replacing the benzyloxycarbonyl group present in **3** by a substituted coumarin in **44** did not significantly alter activity. In contrast, the Fmoc-Cys(substituted coumarin)-OH **45**–**47** had better activities than the cysteine analog Fmoc-Cys(pMeOBzl)-OH **20** (Figure 3, red dotted line) or the lysine analog **3** (brown line), showing the length of the side-chain is not critical for recognition.

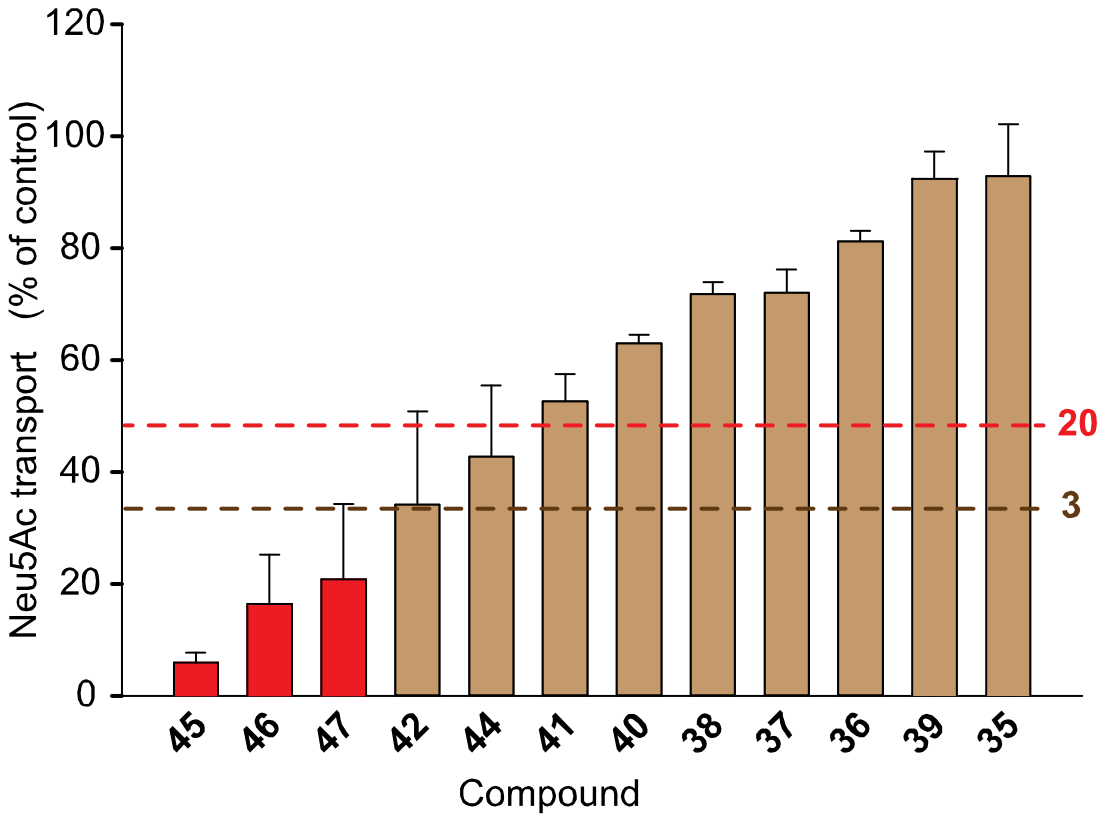

Figure 3. Screening of heterocycle-substituted amino acids. Compounds (30 μM) were tested for inhibition of human sialin as in Figure 1. Each derivative is colored according to, and compared with (dotted lines), its reference compound, **3** (brown) or **20** (red).

The most active compounds **11**, **13**, **45**–**47** inhibited Neu5Ac uptake by sialin in a concentration-dependent manner (Figure 4), in agreement with a specific interaction. Fmoc-Cys[Coum-7-OH]-OH **45** (LSP12-3129) was the most potent inhibitor with an IC_{50} of 2.4 ± 0.7 μM (n = 3), a value ~400-fold lower than the K_M for Neu5Ac.[33] To assess its selectivity, compound **45** was tested on two other H^+-driven lysosomal transporters, LYAAT1 and cystinosin, measured in whole-cell assays similar to that of sialin.[46,47] Interestingly, it had no effect on LYAAT1 and partially inhibited cystinosin (43.7 ± 9.1% inhibition, n = 3) at a concentration (30 μM) that fully inhibits sialin (Figure 4C, D).

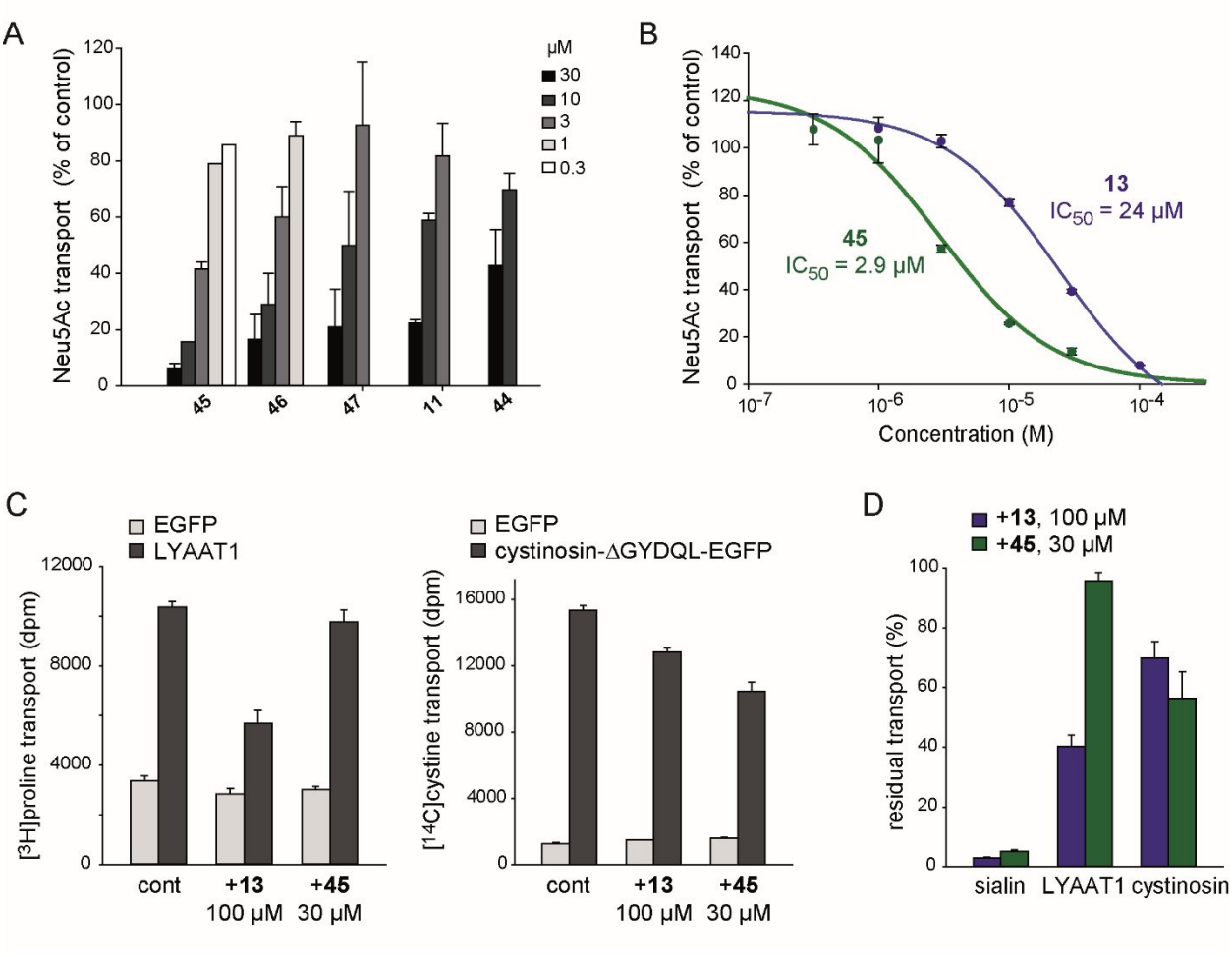

Figure 4. Dose-response relationship and selectivity of selected compounds. (A) Inhibition of human sialin. Means ± SEM of 2-3 independent experiments. (B) Representative sialin inhibition curves for compounds **13** (blue) and **45** (green) (triplicate measurements). (C, D) Effect of **13** and **45** on two other H^+-driven transporters, LYAAT1 and cystinosin. (C) Representative experiments (triplicate measurements). (D) Means ± SEM of 3 independent experiments where the 3 transporters were assayed in parallel.

Compounds 45 and 13 (Fmoc-Leu-OH) are non-competitive inhibitors. We next studied how **45** and, for comparison, **13** (Fmoc-Leu-OH) interact with human sialin. Fmoc-Leu-OH was

chosen because it efficiently inhibits Neu5Ac uptake (Figure 4B; IC_{50} = 23.3 ± 3.5 μM, n = 4) and is commercially available as a radiolabeled compound. Of note, Fmoc-Leu-OH had limited effects on LYAAT1 and cystinosin at a concentration (100 μM) that fully inhibit sialin (Figure 4C, D). We first asked whether these compounds are substrates (translocated ligands) or blockers (not translocated) of the lysosomal transporter. When sialin-expressing cells (EGFP-Sialin L22G/L23G construct) and mock cells (EGFP) were incubated with [^{3}H]Neu5Ac or [^{3}H]Fmoc-Leu-OH at similar saturation levels (IC_{50}/10, corresponding to 100 and 2 μM, respectively), no sialin-dependent [^{3}H]Fmoc-Leu-OH uptake could be detected in acidic medium, in contrast with the strong [^{3}H]Neu5Ac uptake signal (Figure S1). Fmoc-Leu-OH thus acts as a blocker of sialin rather than a translocated substrate.

To extend these experiments to **45**, we developed another whole-cell assay where sialin activity is detected by the co-transport of H^+. We co-expressed the ratiometric fluorescent pH probe E^{2}GFP [48] with a mRFP-tagged human sialin L22G/L23G construct in HEK293 cells to detect the cytosolic acidification associated with the uptake of sialin substrates. Neu5Ac (10 mM) applied at pH 5.5 induced a significant E^{2}GFP fluorescence response consistent with the expected acidification. In contrast, a saturating concentration (30 μM) of **45** did not induce any detectable acidification (Figure S2). Therefore, neither Fmoc-Leu-OH nor **45** are significantly translocated by human sialin, implying they both act as blockers.

We next determined the inhibition mode of these compounds and studied the saturation kinetics of [^{3}H]Neu5Ac uptake at varying inhibitor concentrations. Unexpectedly, despite the 'active site' focus of our initial virtual screening, both Fmoc-Leu-OH and **45** acted as non-competitive rather than competitive inhibitors since they decreased the V_{max} of uptake while leaving the K_M for Neu5Ac essentially unchanged (see representative experiments in Figure 5A and 5B). At 10 μM,

Fmoc-Leu-OH decreased V_{max} by 56 ± 5% (n = 5 independent experiments) with K_M values of 1.6 ± 0.3 and 1.3 ± 0.2 mM in the absence and presence of inhibitor, respectively. Similarly, 45 (3 μM) decreased Vmax by 31 ± 8% (n = 3), with K_M values of 1.4 ± 0.5 and 1.7 ± 0.5 mM in the absence and presence of inhibitor. Mean K_i values of 10.2 ± 3.0 μM (n = 3) and 7.8 ± 1.8 μM (n = 4) were obtained for Fmoc-Leu-OH and **45**, respectively.

Potential mechanism for the non-competitive inhibition. Conceivably, the non-competitive inhibition by Fmoc-Leu-OH and **45** could reflect a decrease in the H^+ electrochemical gradient driving Nue5Ac uptake by sialin. However, the lack of effect of **45** on LYAAT1 and the moderate inhibition of cystinosin by Fmoc-Leu-OH (Figure 4C, D) ruled out this possibility. As our virtual screening was conducted on a cytosol-facing model of sialin,[33] we reasoned that the lack of competition between Neu5Ac, on one hand, and **45** or Fmoc-Leu-OH, on the other hand, might result from a selective blockade of sialin in cytosol-facing state. Like any secondary active transporter,[49,50] sialin should operate through alternating-access structural transitions which expose the substrate binding site to either the luminal (extracellular in our assay) or the cytosolic side of the membrane.[51] If an inhibitor binds to the Neu5Ac-binding site of the outward-facing conformation (Figure 5C, inhibitor 1), the inhibitor and Neu5Ac should exclude each other and an excess of Neu5Ac should displace the inhibitor binding equilibrium, and rescue inhibition. In contrast, if the inhibitor permeates the cell membrane (for instance, by diffusing across the lipid bilayer) and binds to the inward-facing state, the competition between Neu5Ac (on the extracellular side) and the inhibitor (on the cytosolic side) should be biased toward inhibitor binding (Figure 5C, inhibitor 2) because structural transitions are much slower than binding equilibriums: when the cytosolic inhibitor dissociates, the protein in apo, inward-facing state will

rebind another inhibitor molecule before it can switch to the apo, outward-facing state. Extracellular Neu5Ac thus cannot displace the inhibitor binding equilibrium in this case, resulting in non-competitive inhibition. The non-competitive inhibition of sialin by Fmoc-Leu-OH and **45** may thus result from their selective, or preferential, binding to the cytosol-facing state. It may be noted that Fmoc-Leu-OH does enter cells in a sialin-independent manner (Figure S1), enabling its action on the cytosolic side of the transporter.

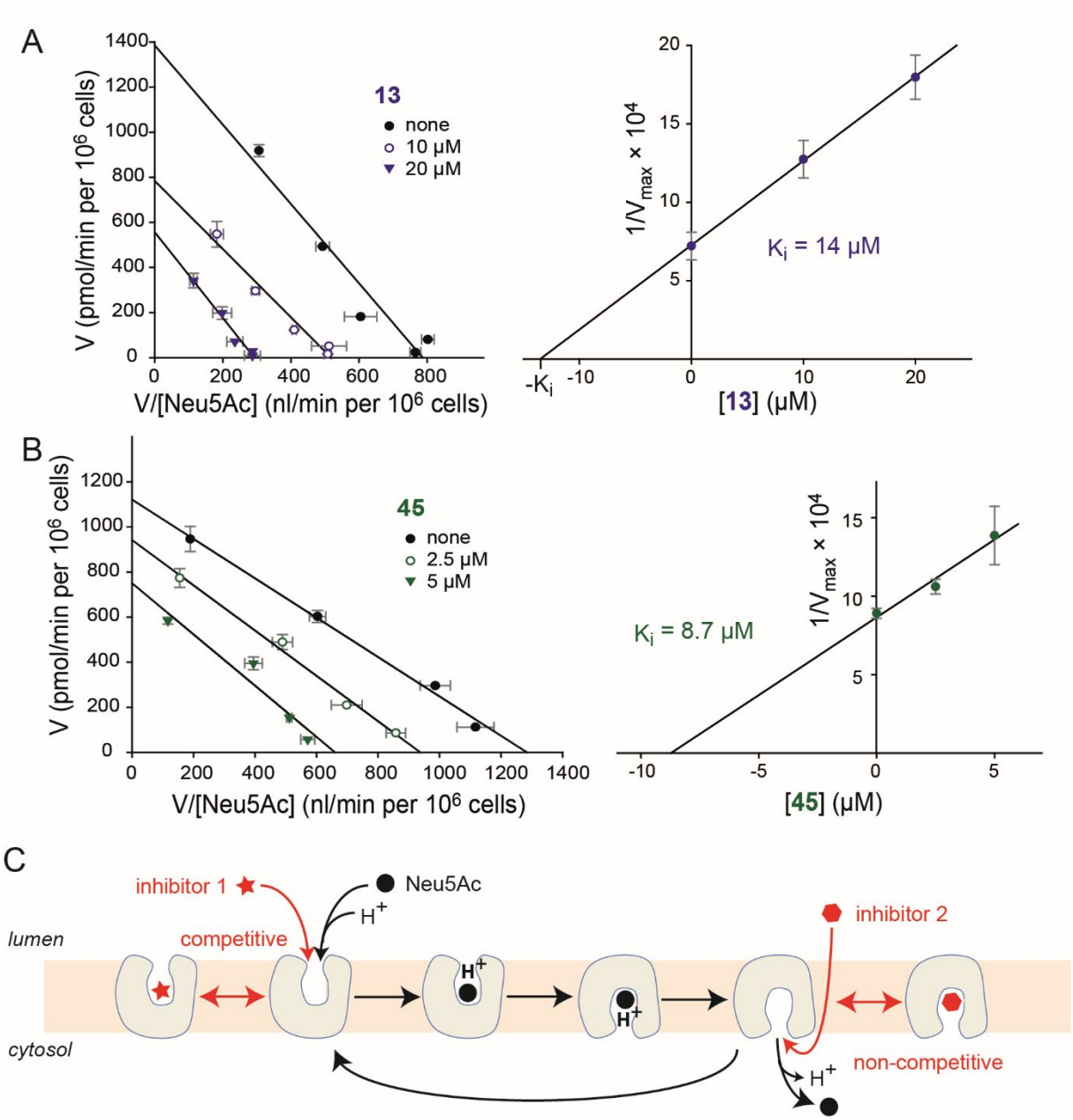

Figure 5. Inhibition mode of Fmoc-Leu-OH and **45**. (A, B) Representative Eadie-Hofstee graphs (left) of [^{3}H]Neu5Ac uptake saturation kinetics in presence or absence of Fmoc-Leu-OH **13** and **45** (means ± SEM of triplicate measurements). The reciprocal maximal velocity is plotted against inhibitor concentration (right graphs) to determine inhibition constants. (C) Potential mechanism accounting for the non-competitive inhibition by aromatic *N*-substituted amino acids (inhibitor 2).

Black arrows depict the Neu5Ac transport cycle in our assay. Red arrows depict two inhibition mechanisms.

We used two approaches to test this model. First, we examined how fast sialin recover its transport activity upon washing of *N*-substituted amino acid inhibitors. If these inhibitors act on the extracellular side, washing should quickly restore Neu5Ac transport. On the contrary, if they predominantly act on the cytosolic side, recovery should be rate-limited by the cellular efflux of cytosolic inhibitors. Cells expressing sialin at the plasma membrane were thus preincubated with Neu5Ac or *N*-substituted amino acids at pH 5.0, washed at neutral pH and tested for [^{3}H]Neu5Ac uptake at pH 5.0 in the absence of inhibitor. For comparison, another set of cells was inhibited during [^{3}H]Neu5Ac uptake, as done previously. When this protocol was applied to Neu5Ac **1**, the neutral wash fully restored [^{3}H]Neu5Ac transport to a level (130%) above that of the uninhibited control, probably reflecting the trans-stimulation of sialin by the cytosolic pool of Neu5Ac accumulated during the pre-incubation step (see ref.[52] for a similar trans-stimulation in lysosomal membrane vesicles). In contrast, when sialin was pre-inhibited by Fmoc-Leu-OH or **45**, only partial recovery was achieved after a 15-min wash (55% and 49% persisting inhibition, respectively) (Figure 6), in agreement with our hypothesis of an action on the cytosolic, rather than the extracellular, side of the transporter. Of note, when this experiment was repeated with FR139317 **2**, which inhibits sialin in a competitive manner[33], the 15-min wash fully restored [3H]Neu5Ac transport without trans-stimulation (Figure S3). The competitive vs. noncompetitive nature of sialin inhibitors thus correlates with the rate of Neu5Ac transport recovery upon washing, in agreement with an action on distinct sides of the membrane. The lower lipophilicity of

FR139317 (logP = 2.29 in protonated state) as compared to Fmoc-Leu-OH and **45** (logP = 4.1 and 3.91, respectively) is also consistent with this model.

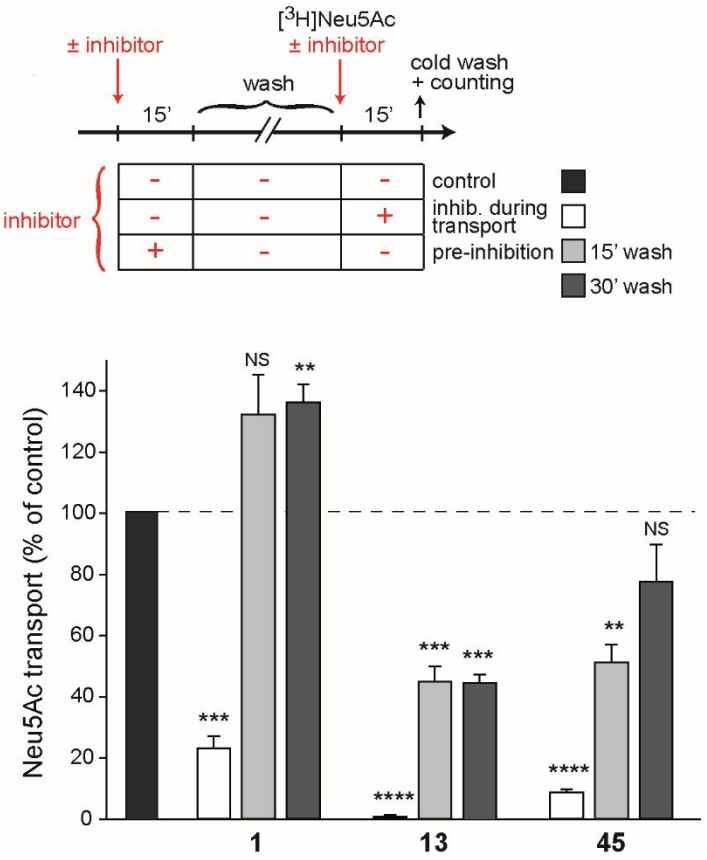

Figure 6. Persistence of **13**- and **45**-induced inhibition upon washing. HEK293 cells expressing sialin at the plasma membrane were pre-incubated or not with Neu5Ac **1** (5 mM), Fmoc-Leu-OH **13** (120 µM) or **45** (12 µM) for 15 min at pH 5. After 15- or 30-min wash at pH 7 at room temperature, [^{3}H]Neu5Ac uptake was measured and compared to the signals obtained in absence or presence of competitors at the same concentrations (means ± SEM of 4 independent experiments). *t*-test relative to control: **= $p<0.01$; *** = $p<0.001$; **** = $p<0.0001$; NS, ≥ 0.05).

Secondly, we examined the docking of **45** to a novel 3D homology model of human sialin based on a closer template. Very recently, two crystal structures of E. coli H+/D-galactonate symporter (DgoT) in outward-facing occluded and inward-facing open conformations have been determined[51]. DgoT is a closer homologue of human sialin (25.5% sequence identity and 45.0% similarity over 420 amino acids; BlastP alignment) than *E. coli* GlpT (21.0% identity and 37.9 similarity over 309 amino acids). Moreover, the DgoT structures have a higher resolution and a better global model quality estimation than the GlpT structure[34,51]. Accordingly, we built two new sialin homology models based on the inward-facing open (6E9N) and outward-facing occluded (6E9O) conformations of DgoT and performed docking experiments with flexible side-chains located at the potential binding site, using GOLD software[53] as implemented in Discovery Studio 2019.

45 could not be docked to the outward-facing occluded sialin model because the binding site was too small to accommodate the inhibitor. In contrast, **45** was well accommodated in the binding site of the inward-facing model (Figure 7A), providing a putative structural explanation for the non-competitive inhibition by this compound. The selected pose was further submitted to a 20-ns molecular dynamics simulation in a membrane environment to optimize the 3D structure.

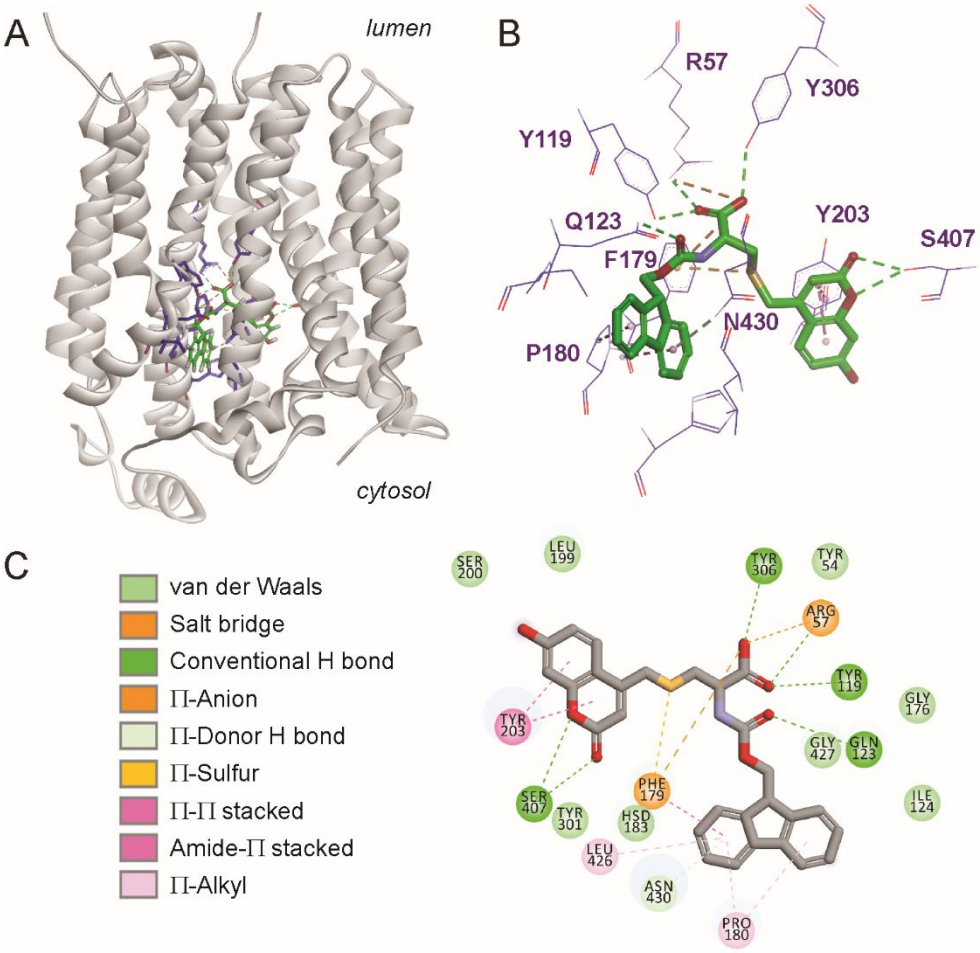

Figure 7. Docking of **45** to a DgoT-based homology model of human sialin. (A) Side view of the inward-facing homology model with the docked inhibitor (in green). (B, C) Residues involved (purple in B) and nature of their interaction with **45** shown in a 2D-depiction.

The interaction of **45** with the inward-facing sialin model is depicted in Figure 7B, C. The carboxylic group of sialic acids and sialin inhibitors, a feature shared with all substrates of SLC17 transporters, is bound to a conserved arginine (R57 in sialin) and two tyrosine (Y119 and Y306). Similar interactions of D-galactonate with this conserved arginine (R47) and two other tyrosine (Y44, Y79) are essential for substrate recognition and selectivity in DgoT.[51]

Two hydrophobic moieties of **45** are expected to block the alternating-access transition of the transporter: a Fmoc group on the amino function of the cysteine core and a coumarinyl group on the side chain of that amino acid. On one side, the 9*H*-fluorene part of the Fmoc group makes hydrophobic interactions with F179, P180, L426 and several van der Waals contacts with I124, H183, G427 and N430. The carbonyl of the Fmoc group establishes a hydrogen bond with Q123. On the other side of the ligand, the coumarinyl group forms hydrogen bonds with S407, a Π stacking with Y203 and van der Waals contacts with L199 and Y301. In between, F179 contacts the sulfur atom and the carboxylate (Figure 7B, C). In MFS transporters, helical discontinuities in specific TMs act as molecular hinges for the rotation of the N and C domains during alternating-access transitions[49]. In DgoT, TM4 has a kink at P135 (P180 in sialin) and TM10 is continuous in the outward-facing conformation whereas TM4 is continuous and TM10 has a kink in the inward-facing conformation[51]. The tight interactions of **45** with residues close to these kinks (Y179, P180 in TM4; S407 in TM10) in the sialin model should block alternating-access movements, providing an explanation for its inhibition of Neu5Ac transport.

Compound 45 partially rescues the sialin R39C mutant. The R39C mutation causing Salla disease induces a trafficking defect of sialin[6,27] possibly due to its destabilization and its recognition by chaperones of the protein quality control system. We reasoned that **45** binding to the cytosolic side of sialin might stabilize nascent R39C polypeptides in the endoplasmic reticulum and rescue their delivery to lysosomes.

45 (12 μM) efficiently inhibited the residual transport activity of sialin R39C in our whole-cell assay (Figure S4), showing **45** binding is not impaired by the pathogenic mutation. We thus transiently expressed wild-type (WT) or R39C human sialin fused to EGFP (with an intact sorting

motif) in HeLa cells in the absence or presence of **45** (70 μM) and examined their intracellular distribution by fluorescence microscopy. As this distribution varies across cells in a given condition (Figure 8A), sialin was compared to a lysosomal marker (LAMP1) and the dual staining in individual cells was classified into three categories: lysosomal (≥70% overlap between sialin and LAMP1 puncta); non-lysosomal (≤30% overlap); and mixed. In agreement with earlier studies, the lysosomal category predominated in untreated cells expressing WT sialin (83%) whereas this category dropped to 11% for the R39C mutant with a predominance of the mixed (55%) and non-lysosomal (34%) categories. However, when sialin R39C was expressed in the presence of **45** (72 μM), the lysosomal category increased to 32% at the expense of the non-lysosomal category (15%) while this treatment did not alter the distribution of WT sialin (Figure 8B). Similar results were observed when sialin was expressed by lipofection instead of electroporation (Figure S4). **45** thus partially rescues the trafficking defect of the R39C mutant. To confirm this effect, we repeated these experiments and quantitated the colocalization between EGFP-sialin and LAMP1 using scatter plots and Pearson's correlation coefficient analysis of the fluorescence intensities. This analysis showed a much lower level of sialin R39C/LAMP1 colocalization relative to the wild-type. When sialin R39C-expressing cells were treated with a high dose (300 μM) of **45**, colocalization was rescued to a level close to that of the wild-type (Figure 8C).

Next, we tested whether this increased delivery of sialin R39C to lysosomes could decrease sialic acid storage in patient cells. We used Salla fibroblasts from a compound-heterozygote patient (R39C and L336W+frameshift alleles) because these cells accumulate sialic acid to higher levels than homozygous R39C cells.[54] Compound-heterozygote Salla fibroblasts and control fibroblasts were thus treated, or not, with **45** (30 to 170 μM) for 2 days and their level of free sialic acid was

assayed by mass spectrometry. Salla fibroblasts cultured in standard medium accumulated free sialic acid ~8-fold as compared to control fibroblasts. The **45** treatment did not reduce, but instead slightly increased, this accumulation (Figure 8C), probably reflecting an inhibition of sialin R39C by **45** at the lysosomal membrane. To circumvent this effect, we used a pulse-chase protocol in which the drug was applied for 2 days to correct the trafficking defect followed by a 6-hr chase in drug-free medium to remove lysosomal inhibition. However, this treatment did not reverse sialic acid storage (data not shown).

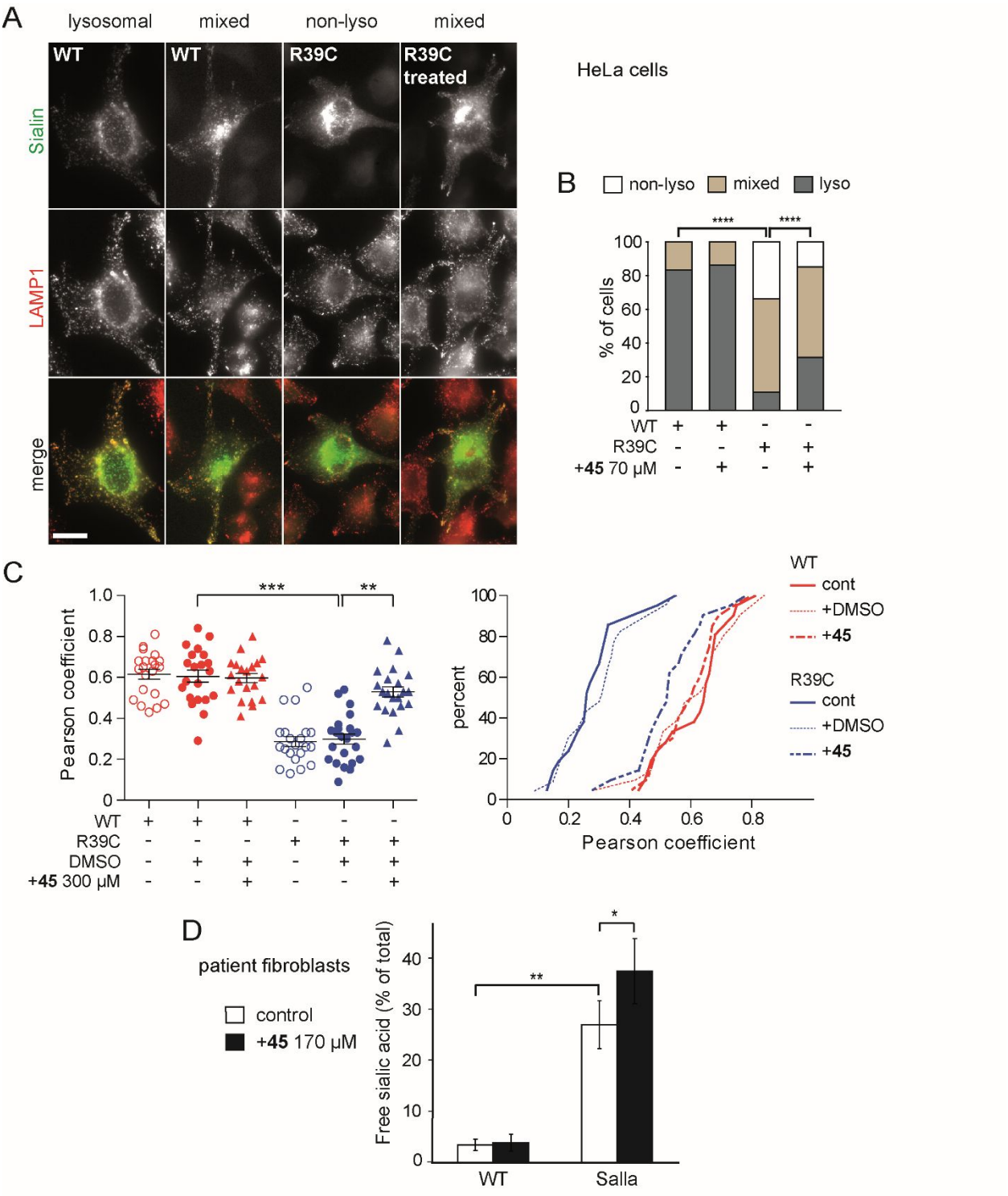

Figure 8. Effect of compound **45** on the R39C mutant. (A, B) Wild-type or R39C human sialin tagged with EGFP was transiently expressed in HeLa cells by electroporation in the presence or absence of **45** (70 µM). After two days, cells were fixed and analyzed under fluorescence

microscopy using LAMP1 immunostaining (red) to detect late endosomes and lysosomes. Sialin localization was categorized as illustrated in (A) in a blind manner. The graph (B) synthesizes the outcome of 3 independent experiments (162 to 184 cells per condition; χ^2 test: ***, $p<0.001$; ****, $p<0.0001$). (C) In independent experiments, colocalization was quantitated using scatter plots of the sialin and LAMP1 pixel intensities. The graphs show the distribution of Pearson's correlation coefficient across 20 to 25 cells per condition in a representative example of three independent experiments (Kruskal-Wallis one-way ANOVA with post hoc Dunn's test: **, $p<0.01$;***, $p<0.001$). (D) Skin fibroblasts from a healthy subject (WT) and a compound heterozygote (p.Arg39Cys/Leu336Trpfs) Salla patient were cultured for 2 days with or without **45** (170 μM) and assayed for free sialic acid level by micro-LC/ESI MRM-MS3 (means ± SEM of 4 independent experiments; *t*-test: * = $p<0.05$; ** = $p<0.01$).

DISCUSSION

In this study, we exploited our previous virtual screening of human sialin[33] and report chemical substitutions of validated virtual hits. This led to the identification of a novel ligand scaffold unrelated to sugar substrates, which is characterized by an amino acid backbone, a free carboxylate, an *N*-linked aromatic or heteroaromatic substituent and a hydrophobic side chain.

Two ligands with this scaffold, Fmoc-Leu-OH **13** and **45**, were characterized in more detail. They inhibited Neu5Ac transport with IC_{50} of 23 and 2.4 μM, respectively, as compared to an IC_{50} of ~1 mM for Neu5Ac. Neither compound was translocated by sialin (Figures S1 and S2) and, somewhat surprisingly, both inhibited Neu5Ac transport in a non-competitive, rather than a competitive, manner (Figure 5), notwithstanding the substrate-binding pocket focus of our virtual

screening.[33] In contrast, another sialin inhibitor identified in this screen, the endothelin-A receptor antagonist FR139317, inhibited Neu5Ac transport in a competitive manner.[33]

This apparent paradox could be explained in a model where the new compounds permeate biological membranes and bind to sialin in cytosol-facing (inward-facing) rather than lumen-facing (outward-facing) conformation. The protonation of the carboxylate group at pH 5.0 and the high partition coefficient of these compounds facilitate their passive diffusion into the cells in our assay of sialin transport activity. As structural transition equilibriums are slower than ligand binding equilibriums, this mechanism should trap sialin in an inward-facing state (Figure 5C) and prevent extracellular Neu5Ac binding to the lumen-facing state, thus decreasing the transport capacity. A similar non-competitive inhibition of a transporter by ligands of the substrate pocket has been reported for the interaction between the glucose transporter GLUT1 and cytochalasin B or forskolin.[55] An analogous mechanism also occurs in enzymes undergoing a conformational change when inhibitors selectively bind the product-favoring conformation.[56] Selective, or predominant, binding of Fmoc-Leu-OH and **45** to an inward-facing state of sialin may thus account for their non-competitive inhibition.

We provide two pieces of evidence in support of this hypothesis. First, inhibition of sialin by Fmoc-Leu-OH and **45** in our whole-cell assay persisted after a 15-min wash (Figure 6), in agreement with an action in the cytosolic rather than the extracellular compartment. Second, we built a more accurate inward-facing homology model of human sialin based on the recent crystallographic structures of the H^+/D-galactonate symporter DgoT[51]. Molecular docking of **45** to this model showed that it binds well to the substrate pocket of the inward-facing state, in agreement with our model. However, other potential mechanisms for the non-competitive inhibition such as

the existence of another **45**-binding site cannot be excluded. Further studies are needed to distinguish between these possibilities.

The best docked pose of **45** showed several interesting features, including an interaction of its carboxylate group with a conserved arginine in TM1 (R57 in human sialin) that is required for D-galactonate binding in DgoT[51]. **45** may thus share common interactions with the anionic substrates of sialin. Another notable feature is the interaction of **45** with residues in TM4 and TM10 that act as hinge regions for alternating-access structural transitions in DgoT[51]. **45** binding to human sialin should thus impair its structural transitions, explaining why this compound blocks Neu5Ac transport.

The identification of **45** as cell-permeant ligand of the 'active' site (sialic acid pocket) of sialin prompted us to test whether it might act as a pharmacological chaperone proof-of-principle for the treatment of Salla disease. Pharmacological chaperones are selective ligands that bind to, and stabilize, misfolded mutant proteins to rescue their retention by the protein quality control system.[57,58] This approach is a promising option for Salla disease as this condition is almost exclusively caused by a single mutation, R39C,[18] which partially preserves the lysosomal targeting and the transport activity of sialin.[6,7] We thus applied **45** to sialin R39C-transfected cells and to Salla patient fibroblasts to test its potential benefits. Interestingly, this treatment partially rescued the trafficking defect of sialin R39C. However, it did not rescue sialic acid storage in patient fibroblasts, presumably because the rescue of the trafficking defect remained insufficient and/or this effect was masked by the inhibition of sialin R39C at the lysosomal membrane. The slight increase of sialic acid storage upon **45** treatment supports the latter hypothesis. In this respect, the

lack of competition between Neu5Ac accumulated in the lumen of patient lysosomes and **45** binding at the cytosolic face of sialin would be a disadvantage for therapeutic applications.

In summary, our study identifies a new class of cell-permeant inhibitors with a micromolar affinity for sialin, providing valuable tools to study the diverse transport activities of sialin and their physiological roles. These tools may also help mechanistic and structural studies of sialin. They may also be used to prevent Neu5Gc incorporation into therapeutic glycoproteins produced by cell culture. In the case of Salla disease, however, further studies are needed to explore the potential of pharmacological chaperone therapy.

EXPERIMENTAL SECTION

General Chemistry Information. All the amino acids belong to the L-series unless specified otherwise. Amino acid derivatives are designated according to the three-letter code and the recommendations from the IUPAC-IUB Commission on Biochemical Nomenclature. Fmoc-Lys(Cbz)-OH **3**, Fmoc-Leu-OH **13**, Fmoc-Asp(tBu)-OH **14**, Fmoc-Cys(tBu)-OH **15**, Fmoc-Tyr(tBu)-OH **17**, Fmoc-Phe-OH **18**, Fmoc-Ile-OH **19**, Fmoc-Cys(pMeOBzl)-OH **20**, Fmoc-Thr(tBu)-OH **21** and Fmoc-Pro-OH **23** were purchased from Novabiochem and used for biological test. Glu(OMe)-OH, DL-Leu-OH, Fmoc-Cys(Trt)-OH, Cys(Bzl)-OH, Fmoc-Lys(Boc)-OH, and HCl.Lys(Cbz)-OMe were purchased from Novabiochem and functionalized. The other reagents were purchased from Aldrich or Acros. Prior to use, tetrahydrofuran (THF) was distilled from sodium-benzophenone and dichloromethane (CH_2Cl_2) from CaH_2. All reactions were carried out under argon atmosphere, and were monitored by thinlayer chromatography with Merck 60F-254 precoated silica (0.2 mm) on glass. Flash chromatography was performed with Merck Kieselgel 60 (200–500 mm); the solvent systems were given v/v. ^{1}HNMR (500 MHz) and ^{13}C NMR (126 MHz) spectra were recorded on a Bruker AVANCEII-500 spectrometer. Chemical shifts (δ) are reported in ppm. Multiplicity was given using the following abbreviations: s (singulet), brs (broad singulet), d (doublet), dd (doublet of doublets), t (triplet), q (quadruplet), m (multiplet). During acquisition, the spectral window covers a proton chemical shift range from –1 to +12 ppm or from –5 to +20 ppm. ^{13}C chemical attributions were assigned using ^{1}H-decoupled spectra. For clarity, in some case, Greek letters are used as locants for NMR attribution of the side chain of the amino acid while the heterocycle moiety is numbered according to the IUPAC Nomenclature. Melting points were determined with a Büchi 530 apparatus and are uncorrected. Mass spectra (MS) were recorded on a Thermo Finnigan LCD Advantage spectrometer and HRMS

on an Exactive (Thermo Scientific) spectrometer with positive (ESI^+) or negative (ESI^-) electrospray ionization. HPLC analyses were carried out on a Prominence Shimadzu instrument, with a LC20A pump, C18 column (250 mm × 4.6 mm, 5 μm), flow: 1 mL/min, eluted peaks were detected by a PDA detector (SPD-M20A), and retention times are reported in minutes. The dead volume is about 200 μL. Products were eluted with method A-1, using solvent A (KH_2PO4 buffer 50 mM, pH 5.5) and solvent B (CH_3CN): 0% B for 10 min, linear increase from 0 to 50% B between 10 and 25 min or with method A-2, using solvent A (KH_2PO_4 buffer 50 mM, pH 5.5) and solvent B (CH_3CN): 0% B for 5 min, linear increase from 0 to 50% B between 5 and 20 min. HPLC-MS analyses were performed on a Surveyor HPLC system coupled to a LCQ Advantage Thermo Finnigan LCQ Advantage Instrument. HPLC was equipped with a Gemini C18 column (100 mm × 2.1 mm, 3 μm), flow: 220 μL/min. The dead volume was about 800 μL. Products were eluted with method B, using solvent A (H_2O/0.1% HCO_2H) and solvent B (MeOH): 40% B for 1 min, linear increase from 40 to 100% B between 1 and 9 min, 100% B from 10 to 13 min, and with method C, using solvent A (H_2O/0.1% HCO_2H) and solvent B (CH_3CN/0.1% HCO_2H): 40% B for 1 min, linear increase from 40 to 100% B between 1 and 6 min, 100% B from 7 to 13 min. Purity of the tested compounds was established by analytical HPLC-MS and HPLC and was at least 95%. Spectroscopic (^1H and ^{13}C NMR, MS) and/or analytical data were obtained using chromatographically homogeneous samples. The photophysical properties of the final compounds were obtained by different measurements on the Greiner and Nonchuk 96-well plates using a Tecan spectrofluorometer (Safire). These measurements were carried out in solution in ethanol at 25 °C.

Syntheses. *General Procedure A for the Synthesis of Compounds **29**, **30** and **31**.* A 0.5 M solution of $ClTi(OiPr)_3$ (1.5 eq) in dry toluene was added to aminophenol (1 eq) and β-cetoester (1 eq) derivatives. The reaction mixture was refluxed overnight, then cooled to room temperature

and diluted with CH_2Cl_2 (7.5 mL/mmol). The whole solution was poured into H_2O (10 mL/mmol) and stirred for few min. The aqueous layer was extracted twice with CH_2Cl_2 (2×30 mL/mmol). The combined organic layers were dried (Na_2SO_4) and the solvent was removed under vacuum. The crude product was purified or used directly to another reaction as mentioned in each case.

*General Procedure B for the Synthesis of Compounds **37–39**, **41** and **44**.* Heteroaromatic derivative (1 eq), amino acid derivative (1–1.2 eq) and HBTU (1.1–1.2 eq), were suspended in CH_2Cl_2 (0.1 M), then DIEA (4-6 eq) was added dropwise at 0 °C and the reaction mixture was stirred for 2 h at room temperature. The solution was diluted with CH_2Cl_2 (50 mL/mmol) and washed three times with aqueous HCl solution (0.1 M, 20 mL/mmol). Aqueous layers were extracted twice with CH_2Cl_2 (50 mL/mmol), then the organic layers were pooled, dried (Na_2SO_4), filtered and evaporated. The mixture was treated with aqueous LiOH solution (0.5 M, 1.2 eq)/THF (1/1) and stirred for 2 h at room temperature. The solution was evaporated and diluted with H_2O, then acidified to pH 2 with HCl (1 M). The precipitate was filtered and, when necessary, purified by column chromatography on silica gel (CH_2Cl_2/MeOH/AcOH: 95/5/0.1 to 85/15/1).

*4-Carboxymethyl-7-dimethylamino-coumarin (**29**).* The *General Procedure A* was followed using $ClTi(O\textit{i}Pr)_3$ (1.791 mL, 7.5 mmol) in toluene (12 mL), 3-dimethylaminophenol (0.685 g, 5 mmol) and dimethyl 3-oxoglutarate (1.791 mL, 5 mmol). The crude product was dissolved in MeOH (12.5 mL) and in aqueous NaOH solution (1 M, 12.5 mL) and stirred overnight at room temperature. The solution was acidified to pH 5 with aqueous HCl solution (2 M) and the resulting precipitate was recovered by filtration, washed with HCl (0.1 M) and dried under vacuum. Compound **29** (0.487 g) was obtained as a green-yellow powder in 40% yield. ^{1}H NMR (500 MHz, $(CD_3)_2SO$): δ 7.47 (d, J = 9.0 Hz, 1H, H-5), 6.72 (dd, J = 9.0 Hz, J = 2.5 Hz, 1H, H-6), 6.56 (d, J = 2.5 Hz, 1H, H-8), 6.05 (s, 1H, H-3), 3.77 (s, 2H, CH_2), 3.01 (s, 6H, CH_3); ^{13}C NMR (126 MHz,

$(CD_3)_2SO$): δ 170.7 (CO_2H), 160.6 (C=O), 155.4 (Cq-O), 152.8 (Cq-Ar), 150.2 (Cq-N), 126.0, 109.6, 109.1 (CH-Ar), 108.0 (Cq-Ar), 97.5 (CH-Ar), 40.1 (2×NCH_3), 37.2 (CH_2); MS: (ESI^+), m/z (%): $[M + H]^+$ = 248.3 (100%); $[2M + Na]^+$ = 517.0 (80%); $\lambda_{abs}^{max} =$ 373 nm, $\lambda_{em}^{max} =$ 443 nm, ε (λ_{max}) = 23300 $M^{-1}cm^{-1}$, Φ = 0.677.

*4-Carboxymethyl-7-diethylamino-coumarin (**30**)*. The *General Procedure A* was followed using $ClTi(OiPr)_3$ (3.582 mL, 15 mmol) in toluene (25 mL), 3-diethylaminophenol (1.652 g, 10 mmol) and dimethyl 3-oxoglutarate (1.470 mL, 10 mmol). The crude product was dissolved in MeOH (25 mL) and in aqueous NaOH solution (1 M, 25 mL), then stirred overnight at room temperature. The solution was acidified to pH 5 with aqueous HCl solution (2 M) and the resulting precipitate was recovered by filtration, washed with HCl (0.1 M) and dried under vacuum. Compound **30** (0.947 g) was obtained as a green powder in 35% yield. ^1H NMR (500 MHz, $(CD_3)_2SO$): δ 7.44 (d, J = 9.0 Hz, 1H, H-5), 6.69 (dd, J = 9.0 Hz, J = 2.5 Hz, 1H, H-6), 6.51 (d, J = 2.5 Hz, 1H, H-8), 5.99 (s, 1H, H-3), 3.75 (s, 2H, CH_2CO_2H), 3.41 (q, J = 7.0 Hz, 4H, NCH_2), 1.11 (t, J = 7.0 Hz, 6H, CH_3); ^{13}C NMR (126 MHz, $(CD_3)_2SO$): δ 170.7 (CO_2H), 160.7 (C=O), 155.8 (Cq-O), 150.4 (Cq-Ar), 150.1 (Cq-N), 126.3, 109.1, 108.7 (CH-Ar), 107.6 (Cq-Ar), 96.8 (CH-Ar), 44.0 (2×NCH_2), 37.2 (CH_2CO_2H), 12.3 (2×CH_3); MS: (ESI^+), m/z (%): $[M + H]^+$ = 276.3 (100%); $[2M + Na]^+$ = 573.0 (85%); $[2M + H]^+$ = 550.9 (70%).

*2-(11-Oxo-2,3,6,7-tetrahydro-1H,5H,11H-pyrano[2,3-f]pyrido[3,2,1-ij]quinolin-9-yl)acetic acid (31) (**31**)*. From $ClTi(OiPr)_3$ (2.262 mL, 6.75 mmol) in toluene (9 mL), 8-hydroxyjulodin (0.851 g, 4.5 mmol) and dimethyl 3-oxoglutarate (681 µL, 4.5 mmol), compound **31** as methyl ester was obtained, according to *General Procedure A* and used without further purification in the next step. ^1H NMR (500 MHz, $CDCl_3$): δ 6.99 (s, 1H, H-8), 5.98 (s, 1H, H-10), 3.70 (s, 3H, CH_3), 3.61 (s, 2H, $CH_2CO_2CH_3$), 3.26 (q, J = 6.0 Hz, 4H, CH_2-N), 2.89 (t, J = 6.5 Hz, 2H, CH_2-Ph), 2.79

(t, J = 6.5 Hz, 2H, CH_2-Ph), 1.98 (m, 4H, CH_2-CH_2-CH_2). Methyl ester **31** as was then dissolved in MeOH (15 mL) and aqueous NaOH solution (1 M, 15 mL) and the mixture was stirred overnight at room temperature. The pH was adjusted to 2 with aqueous HCl solution (1 M) and the resulting precipitate was recovered by filtration and washed with aqueous HCl solution (0.1 M, 30 mL). Compound **31** (0.890 g) was obtained as a yellow powder in 66% yield. Mp 186–187 °C; ^{1}H NMR (500 MHz, $(CD_3)_2SO$): δ 12.67 (brs, 1H, CO_2H), 7.05 (s, 1H, H-8), 5.94 (s, 1H, H-10), 3.71 (s, 2H, CH_2CO_2H), 3.24 (m, 4H, CH_2-N), 2.71 (m, 4H, CH_2-Ph), 1.88 (m, 4H, CH_2-CH_2-CH_2); ^{13}C NMR (126 MHz, $(CD_3)_2SO$): δ 170.8 (CO_2H), 160.7 (C=O), 150.7, 150.1, 145.5 (Cq-Ar), 122.0 (CH-Ar), 117.7 (Cq-Ar), 108.3 (CH-Ar), 107.4, 105.6 (Cq-Ar), 49.2, 48.6 (CH_2-N), 37.2 (CH_2CO_2H), 27.0, 20.9, 20.0, 19.9 (CH_2); MS: (ESI^+), m/z (%): $[M + H]^+$ = 300.1 (80%); $[2M + Na]^+$ = 621.1 (100%).

*3-(3,6-Dihydroxy-xanthen-9-ylidene)propanoic acid (**32**)*. A stirred mixture of succinic anhydride (2.50 g, 25 mmol, 0.5 eq) and resorcinol (2.75 g, 25 mmol, 1 eq) in aqueous H_2SO_4 solution (70%, 30 mL) was heated to 140 °C for 4 h. The reaction mixture was then cooled to room temperature and poured into H_2O (500 mL). The stirred solution was alkalinized to pH 12 with aqueous NaOH solution (50%), while the temperature was kept at 0 °C. Acetic acid was added to the solution until pH 4, and the resulting brown precipitate was filtered. The filtrate was washed with H_2O (3×25 mL), acetone (15 mL), and dried under reduced pressure to give pure compound **32** (3.28 g) as an orange solid in 92% yield from resorcinol. ^{1}H NMR (500 MHz, $(CD_3)_2SO$): δ 7.51 (d, 1H, J = 8.5 Hz, H-Ar), 7.41 (d, 1H, J = 8.5 Hz, H-Ar), 6.65–6.47 (m, 4H, H-Ar), 5.87 (t, 1H, J = 7.0 Hz, C=CH), 3.31 (d, 2H, J = 7.0 Hz, CH_2-CH); ^{13}C NMR (126 MHz, $(CD_3)_2SO$): δ 173.5 (CO_2H), 158.2, 157.9 (Cq-OH), 153.0, 151.3 (Cq-Ar), 128.6 (CH-Ar), 125.7 (Cq-Ar), 124.3, 116.1 (CH-Ar), 114.0, 113.1 (Cq-Ar), 112.0 (CH-Ar), 110.8 (=CH), 102.6, 102.3 (CH-Ar), 36.3

(CH_2); MS: (ESI^+), m/z (%): $[M + H]^+$ = 285.1 (100%); λ_{abs}^{max} = 455 nm, λ_{em}^{max} = 516 nm, ε (λmax) = 5140 $M^{-1}cm^{-1}$, Φ = 0.243.

*4-Hydroxymethyl-7-methoxymethoxy-coumarin (**33**).* Compound **27** (0.576 g, 3 mmol, 1 eq) was suspended in CH_2Cl_2 at 0 °C. DIEA (272 µL, 3.6 mmol, 1.2 eq) and MOM-Cl (627 µL, 3.6 mmol, 1.2 eq) were added dropwise, and the solution was stirred for 45 min at 0 °C. After evaporation under reduced pressure, H_2O (10 mL) was added to the residue and the resulting precipitate was recovered by filtration and dried under vacuum. Compound **33** (0.511 g) was obtained as a white solid in 71% yield. ^1H NMR (500 MHz, $(CD_3)_2SO$): δ 7.63 (d, J = 8.5 Hz, 1H, H-5), 7.04 (d, J = 2.5 Hz, 1H, H-8), 7.00 (dd, J = 8.5 Hz, J = 2.5 Hz, 1H, H-6), 6.32 (s, 1H, H-3), 5.30 (s, 2H, OCH_2O), 4.72 (s, 2H, CH_2OH), 3.39 (s, 3H, CH_3); ^{13}C NMR (126 MHz, $(CD_3)_2SO$): δ 160.3 (C=O), 159.4 (Cq-7), 156.4 (Cq-4), 154.4 (Cq-8a), 125.4 (CH-5), 113.1 (CH-6), 111.5 (Cq-4a), 103.2, 103.1 (CH-3, CH-8), 93.9 (OCH_2O), 59.0 (CH_2OH), 58.9 (CH_3); MS: (ESI^+), m/z (%): $[M + H]^+$ = 237.1 (100%).

*7-(Methoxymethoxy)-4-(Fmoc-oxymethyl)-coumarin (**34**).* Fmoc-Cl (0.206 g, 0.8 mmol, 1.2 eq) was added by portion over 30 min to a solution of compound **33** (0.160 g, 0.68 mmol, 1eq) in dry pyridine (3 mL). After stirring 2 h at room temperature, the reaction mixture was diluted with EtOAc (20 mL) and washed with brine (3×20 mL). The organic layer was dried, filtered and evaporated under vacuum. The residue was purified by silica-gel column chromatography (cyclohexane/EtOAc: 9/1 to 7/3). Compound **34** (0.108 g) was obtained as a white powder in 34% yield. ^1H NMR (500 MHz, $CDCl_3$): δ 7.75 (d, J = 7.5 Hz, 2H, H-Ar), 7.59 (d, J = 7.5 Hz, 2H, H-Ar), 7.40 (m, 3H, H-Ar), 7.31 (t, J = 6.5 Hz, 2H, H-Ar), 7.03 (d, J = 2.5 Hz, 1H, H-8), 6.97 (dd, J = 9.0 Hz, J = 2.5 Hz, 1H, H-6) 6.38 (t, J = 1.5 Hz, 1H, H-3), 5.29 (d, J = 1.5 Hz, 2H, CH_2–Coum), 5.22 (s, 2H, OCH_2O), 4.48 (d, J = 7.0 Hz, 2H, CH_2CH), 4.26 (t, J = 7.0 Hz, 1H, CH_2C*H*), 3.47 (s,

3H, CH_3); ^{13}C NMR (126 MHz, $CDCl_3$): δ 160.7, 160.6 (C=O, Cq-O), 155.5 (OCO_2), 154.7 (Cq-OMOM), 148.4 (Cq-Ar), 143.2, 141.5 (2×Cq-Ar), 128.2, 127.4, 125.3 (2×CH-Ar), 124.6 (CH-Ar), 120.3 (2×CH-Ar), 113.8 (CH-Ar), 111.5 (Cq-Ar), 111.1, 104.5 (CH-Ar), 94.6 (OCH_2O), 70.7 (CH_2CH), 64.7 (CH_2–Coum), 56.6 (CH_3), 46.9 (OCH_2CH); MS: (ESI^+), m/z (%): $[M + H]^+$ = 459.3 (100%).

7-Hydroxy-4-(Fmoc-oxymethyl)-coumarin ***(35)***. Compound **34** (0.090 g, 0.2 mmol) was supended in CH_2Cl_2 (1.5 mL) at 0 °C and TFA (1.5 mL) was added. The solution was stirred 1.5 h at room temperature. After evaporation of the solvents, the residue was purified by silica gel column chromatography (cyclohexane/EtOAc: 9/1 to 7/3). Compound **35** (0.069 g) was obtained as a white powder in 83% yield. ^1H NMR (500 MHz, $(CD_3)_2SO$): δ 10.63 (s, 1H, OH), 7.89 (d, J = 7.5 Hz, 2H, H-Ar), 7.66 (d, J = 7.5 Hz, 2H, H-Ar), 7.51 (d, J = 8.5 Hz, 1H, H-5), 7.41 (t, J = 7.5 Hz, 2H, H-Ar), 7.32 (t, J = 7.5 Hz, 2H, H-Ar), 6.81 (dd, J = 8.5 Hz, J = 2.5 Hz, 1H, H-6), 6.75 (d, J = 2.5 Hz, 1H, H-8), 6.08 (s, 1H, H-3), 5.33 (s, 2H, CH_2–Coum), 4.61 (d, J = 6.0 Hz, 2H, OCH_2CH), 4.34 (t, J = 6.0 Hz, 1H, OCH_2CH); ^{13}C NMR (126 MHz, $(CD_3)_2SO$): δ 161.4, 159.9, 155.0 (Cq-O), 153.9 (OCO_2), 149.7 (Cq-Ar), 143.2 (2×Cq-Ar), 140.8 (2×Cq-Ar), 127.7, 127.1 (2×CH-Ar), 125.9 (CH-Ar), 124.8, 120.2 (2×CH-Ar), 113.0 (CH-Ar), 108.9 (Cq-4a), 108.4 (CH-3), 102.4 (CH-8), 69.2 (OCH_2CH), 64.6 (CH_2–Coum), 46.3 (OCH_2CH); HPLC–MS (Method B): t_R = 14.1 min; MS: (ESI^+), m/z (%): $[M + H]^+$ = 415.1 (100%); $[2M + Na]^+$ = 850.9 (60%); HRMS (ESI^-) calcd for $[C_{25}H_{18}O_6 - H]^-$: 413.1030; found: 413.1040; λ_{abs}^{max} = 324 nm, λ_{em}^{max} = 399 nm, ε (λmax) = 4760 $M^{-1}cm^{-1}$, Φ = 0.243.

N^6-((Benzyloxy)carbonyl-N^2-(2-(7-hydroxy-2-oxo-2H-chromen-4-yl)acetyl)-L-lysine ***(36)***. 7-Hydroxy-4-carboxymethyl-coumarin (0.220 g, 1 mmol, 1 eq), HBTU (0.417 g, 1.1 mmol, 1.1 eq) and HOBt (0.148 g, 1.1 mmol, 1.1 eq) were diluted in anhydrous DMF (3 mL). DIEA

(380 µL, 2.2 mmol, 2.2 eq) was added dropwise and the resulting solution was stirred few min, then a solution of HCl.Lys(Cbz)-OMe (0.331 g, 1 mmol, 1 eq) in DMF (1 mL) was added. The reaction mixture was stirred overnight at room temperature and DMF was evaporated. The residue was diluted in EtOAc (50 mL), washed with brine (3×40 mL), dried (Na_2SO_4), filtered and evaporated. The ester compound was diluted with THF (4 mL) and a solution of aqueous LiOH (0.5 M, 4 mL) and stirred 2 h at room temperature. After evaporation THF, pH was adjusted to 2 with aqueous HCl solution (1 M) and extracted with EtOAc (2×40 mL). Organic layers were dried (Na_2SO_4), filtered and evaporated. The residue was purified by column chromatography on silica gel (CH_2Cl_2/MeOH/AcOH: 85/15/1). Compound **36** (0.090 g) was obtained as a white powder in 19% yield. Mp 78–79 °C; ^{1}H NMR (500 MHz, CD_3OD): δ 7.47 (d, J = 8.5 Hz, 1H, H-Ar), 7.17 (m, 5H, H-Ph), 6.64 (d, J = 8.5 Hz, 1H, H-Ar), 6.54 (s, 1H, H-Ar), 6.06 (s, 1H, H-Ar), 4.89 (s, 2H, CH_2-Ph), 4.19 (m, 1H, H-α), 3.60 (s, 2H, CH_2—Coum), 2.93 (m, J = 6.5 Hz, 2H, H-ε), 1.70, 1.56 (2m, 2H, H-β), 1.34–1.25 (m, 4H, H-γ, H-δ); ^{13}C NMR (126 MHz, CD_3OD): δ 175.2 (CO_2H), 170.8 (CONH) 163.1, 163.0, 158.9 (CO-Coum), 156.8 ($NHCO_2$), 152.6, 138.7 (Cq-Ar), 129.7 (2×CH-Ar), 129.1 (CH-Ar), 128.9 (2×CH-Ar), 127.9, 114.4 (CH-Ar), 113.2 (CH-Ar, Cq-Ar), 103.8 (CH-Ar), 67.3 (OCH_2-Ph), 66.9 (CH_2—Coum), 54.0 (C-α), 41.6 (C-ε), 32.2 (C-β), 30.6 (C-δ), 24.3 (C-γ); HPLC (Method A-2): tR = 13.2 min; HPLC–MS (Method B): t_R = 11.8 min; MS: (ESI$^+$), m/z (%): $[M + H]^+$ = 483.1 (100%), $[M – CO_2 + H]^+$ = 439.4 (20%); MS: (ESI$^-$), m/z (%): $[M – H]^-$ = 481.3 (100%), $[M – C_7H_8O – H]^-$ = 373.2 (50%); HRMS (ESI$^-$) calcd for [$C_{25}H_{26}N_2O_8$ – H]– : 481.1616; found: 481.1619; λ_{abs}^{max} = 324 nm, λ_{em}^{max} = 399 nm, ε (λmax) = 9880 $M^{-1}cm^{-1}$, Φ = 0.0904.

*N^6-((Benzyloxy)carbonyl-N^2-(2-(7-(dimethylamino)-2-oxo-2H-chromen-4-yl)acetyl)-L-lysine (**37**).* From 7-dimethylamino-4-carboxymethyl-coumarin **29** (0.125 g, 0.5 mmol, 1 eq),

HCl.Lys(Cbz)-OMe (0.165 g, 0.6 mmol, 1.1 eq), HBTU (0.220 g, 0.6 mmol, 1.1 eq) and DIEA (346 µL, 2.0 mmol, 4 eq), compound **37** (0.128 g) was obtained by filtration, as a yellow powder in 50% yield, according to *General Procedure B*. ^{1}H NMR (500 MHz, $(CD_3)_2SO$): δ 8.55 (d, J = 7.0 Hz, 1H, NH), 7.56 (d, J = 9.0 Hz, 1H, H-5), 7.30 (m, 6H, H-Ph, NH), 6.66 (d, J = 9.0 Hz, 1H, H-6), 6.54 (s, 1H, H-8), 6.04 (s, 1H, H-3), 5.00 (s, 2H, CH_2-Ph), 4.16 (m, 1H, H-α), 3.67 (s, 2H, CH_2–Coum), 3.00 (m, 8H, H-ε, CH_3), 1.71, 1.61 (2m, 2H, H-β), 1.39-1.30 (m, 4H, H-γ, H-δ); ^{13}C NMR (126 MHz, $(CD_3)_2SO$): δ 173.4 (CO_2H), 168.0 (CONH) 160.7, 156.0 (CO-Coum), 155.3 ($NHCO_2$), 152.8 (Cq-Ar), 151.3 (Cq-N$(Me)_2$), 137.7 (Cq-Ar), 128.3 (2×CH-Ar), 127.7 (3×CH-Ar), 126.0 (CH-Ar), 109.3 (CH-Ar), 108.9 (CH-Ar), 108.2 (Cq-Ar), 97.5 (CH-Ar), 65.1 (OCH_2-Ph), 52.00 (C-α), 40.1 (C-ε, 2xNCH_3), 38.4 (CH_2–Coum), 30.6 (C-β), 29.0 (C-δ), 22.7 (C-γ); HPLC (Method A-2): t_R = 14.4 min; HPLC–MS (Method B): t_R = 13.7 min; MS: (ESI$^+$), m/z (%): $[M + H]^+$ = 510.1 (100%), $[M - CO_2 + H]^+$ = 466.3 (20%); MS: (ESI$^-$), m/z (%): $[M - H]^-$ = 508.3 (100%): HRMS (ESI$^-$) calcd for $[C_{27}H_{31}N_3O_7 - H]^-$: 508.2089; found: 508.2089; λ_{abs}^{max} = 373 nm, λ_{em}^{max} = 448 nm, Φ = 0.714, ε (λmax) = 16800 $M^{-1}cm^{-1}$.

N^6-((Benzyloxy)carbonyl-N^2-(2-(7-(diethylamino)-2-oxo-2H-chromen-4-yl)acetyl)-L-lysine ***(38)***. From 7-diethylamino-4-carboxymethyl-coumarin **30** (0.275 g, 1.0 mmol, 1 eq), HCl.Lys(Cbz)-OMe (0.360 g, 1.2 mmol, 1.2 eq), HBTU (0.440 g, 1.2 mmol, 1.2 eq) and DIEA (865 µL, 5.0 mmol, 5 eq), compound **38** (0.128 g) was obtained by filtration, as a yellow powder in 19% yield, according to *General Procedure B*. ^{1}H NMR (500 MHz, $(CD_3)_2SO$): δ 8.54 (d, J = 7.5 Hz, 1H, NH), 7.52 (d, J = 9.0 Hz, 1H, H-5), 7.30 (m, 6H, H-Ph, NH), 6.66 (dd, J = 9.0 Hz, J = 2.5 Hz, 1H, H-6), 6.54 (d, J = 2.5 Hz, 1H, H-8), 5.99 (s, 1H, H-3), 5.00 (s, 2H, CH_2-Ph), 4.15 (m, 1H, H–α), 3.65 (s, 2H, CH_2–Coum), 3.41 (q, J = 7.0 Hz, 4H, N(CH_2CH_3)$_2$), 2.96 (m, 2H, H-ε), 1.72, 1.60 (2m, 2H, H-β), 1.45-1.26 (m, 4H, H-γ, H-δ), 1.10 (t, J = 7.0 Hz, 6H, N(CH_2CH_3)$_2$);

^{13}C NMR (126 MHz, $(CD_3)_2SO$): δ 173.4 (CO_2H), 168.0 (CONH), 160.7, 156.0 (CO-Coum), 155.7 ($NHCO_2$), 151.2 (Cq-Ar), 150.3 (Cq-$N(Me)_2$), 137.3 (Cq-Ar), 128.3 (2×CH-Ar), 127.7 (3×CH-Ar), 126.3 (CH-Ar), 108.8 (CH-Ar), 108.5 (CH-Ar), 107.7 (Cq-Ar), 96.8 (CH-Ar), 65.1 (OCH_2-Ph), 52.0 (C-α), 44.0 (2xNCH_2CH_3), 40.1 (C-ε), 38.4 (CH_2–Coum), 30.6 (C-β), 29.0 (C-δ), 22.7 (C-γ), 12.3 (2xNCH_2CH_3); HPLC (Method A-2): t_R = 15.9 min; HPLC–MS (Method B): t_R = 14.7 min; MS: (ESI$^+$), m/z (%): $[M + H]^+$ = 538.1 (100%), $[2M + H]^+$ = 1074.9 (90%), $[M – CO_2 + H]^+$ = 494.4 (20%); HRMS (ESI$^–$) calcd for $[C_{29}H_{35}N_3O_7 – H]^–$: 536.2402; found: 536.2402; λ_{abs}^{max} = 379 nm, λ_{em}^{max} = 446 nm, ε (λmax) = 18600 $M^{-1}cm^{-1}$, Φ = 0.749.

N^6-((Benzyloxy)carbonyl-N^2-(2-oxo-1,2-dihydroquinoline-4-carbonyl)-L-lysine ***(39)***. From 4-carboxy-quinolin-2-one (0.189 g, 1.0 mmol, 1 eq), HCl.Lys(Cbz)-OMe (0.364 g, 1.1 mmol, 1.1 eq), HBTU (0.420 g, 1.1 mmol, 1.1 eq) and DIEA (692 µL, 4 mmol, 4 eq), compound **39** (0.168 g) was obtained, after purification by column chromatography on silica gel (CH_2Cl_2/MeOH/AcOH: 85/15/1), as a white powder in 43% yield, according to *General Procedure B*. Mp 214–215 °C; ^{1}H NMR (500 MHz, $(CD_3)_2SO$): δ 11.94 (brs, 1H, CO_2H), 8.51 (d, J = 7.5 Hz, 1H, H-Ar), 7.80 (d, J = 8.5 Hz, 1H, NH), 7.50 (t, J = 7.5 Hz, 1H, H-Ar), 7.35–7.21 (m, 7H, H-Ar, H-Ph), 7.17 (t, J = 7.5 Hz, 1H, H-Ar), 6.53 (s, 1H, H-Ar), 4.98 (s, 2H, CH_2-Ph), 4.27 (m, 1H, H-α), 2.99 (m, 2H, H-ε), 1.85, 1.64 (2m, 2H, H-β), 1.46–1.34 (m, 4H, H-γ, H-δ); ^{13}C NMR (126 MHz, $(CD_3)_2SO$): δ 173.0 (CO_2H), 165.3 (CONH-Ar), 161.4 (CO-Ar) 156.0 ($NHCO_2$), 146.6 (Cq-Ar), 139.2 (Cq-Ar), 137.3 (Cq-Ar), 130.6 (CH-Ar), 128.3 (2×CH-Ar), 127.6 (3×CH-Ar), 126.2 (Cq-Ar), 121.9 (CH-Ar), 119.5 (CH-Ar), 116.4 (CH-Ar), 115.5 (CH-Ar), 65.1 (OCH_2-Ph), 53.6 (C-α), 40.2 (C-ε), 31.1 (C-β), 29.2 (C-δ), 23.0 (C-γ); HPLC (Method A-2): t_R = 12.8 min; HPLC–MS (Method B): t_R = 11.8 min; MS: (ESI$^+$), m/z (%): $[M + H]^+$ = 452.3 (100%), $[M – CO_2 + H]^+$ = 408.3 (20%); MS: (ESI$^–$), m/z (%): $[M – H]^–$ = 450.6 (20%); $[2M – H]^–$ = 902.0

(100%); HRMS (ESI$^-$) calcd for $[C_{24}H_{25}N_3O_6 - H]^-$: 450.1670; found: 450.1669; $\lambda_{abs}^{max} =$ 332 nm, $\lambda_{em}^{max} =$ 434 nm, ε (λmax) = 16700 $M^{-1}cm^{-1}$, Φ = 0.0101.

*N^6-((Benzyloxy)carbonyl-N^2-(3-(3,6-dihydroxy-9H-xanthen-9-ylidene)propanoyl)-L-lysine (**40**)*. From compound **32** (0.384 g, 1.0 mmol, 1 eq), HBTU (0.417 g, 1.1 mmol, 1.1 eq) and HOBt (0.148 g, 1.1 mmol, 1.1 eq) were diluted with anhydrous DMF (3 mL). DIEA (380 µL, 2.2 mmol, 2.2 eq) was added dropwise and this solution was stirred for few min, then a solution of HCl.Lys(Cbz)-OMe (0.331 g, 1.0 mmol, 1 eq) in DMF (1 mL) was added. The solution was stirred overnight at room temperature then, the solvent was evaporated, and the residue was diluted in EtOAc (50 mL). The organic layer was washed with brine (3×40 mL), dried (Na_2SO_4), filtered and evaporated. The mixture was diluted with a solution of aqueous LiOH (0.5 M)/THF (40 mL, 1/1) and stirred 2 h at room temperature. After evaporation of THF, the pH was adjusted to 2 with aqueous HCl solution (1 M) and extracted with EtOAc (2×40 mL). Organic layer was dried (Na_2SO_4), filtered and evaporated. The residue was purified by column chromatography on silica gel (CH_2Cl_2/MeOH/AcOH: 85/15/1). Compound **40** (0.045 g) was obtained as a red powder in 8% yield. Mp 106–107 °C; ^{1}H NMR (126 MHz, $(CD_3)_2SO$): δ 7.51 (d, J = 8.5 Hz, 1H, H-Ar), 7.41 (d, J = 8.5 Hz, 1H, H-Ar), 7.15 (m, 5H, H-Ph), 6.59–6.45 (m, 4H, H-Ar), 5.78 (t, J = 7.0 Hz, 1H, C=CH), 4.69 (s, 2H, CH_2-Ph), 4.25 (m, 1H, H-α), 3.31 (d, J = 7.0 Hz, 2H, CH_2-CH), 2.88 (m, 2H, H-ε), 1.70, 1.55 (m, 2H, H-β), 1.29–1.18 (m, 4H, H-γ, H-δ); ^{13}C NMR (126 MHz, $(CD_3)_2SO$): δ 172.9 (CO_2H), 164.8 (CONH), 158.2, 157.9 (Cq-3, Cq-6), 156.0 (NHCO), 153.0 (Cq-Ar), 151.3 (Cq-Ar), 138.7 (Cq-Ar), 128.3 (CH-Ar), 128.1 (2xCH-Ar), 127.2 (3xCH-Ar), 125.7 (Cq-Ar), 123.3, 115.7 (CH-Ar), 114.0, 113.1 (Cq-Ar), 112.0 (CH-Ar), 110.8 (=CH), 103.0 (CH-Ar), 102.4 (CH-Ar), 66.1 (OCH_2Ph), 52.6 (C-α), 40.6 (C-ε), 36.3 (CH_2CO), 31.0 (C-β), 29.1 (C-δ), 22.6 (C-γ); HPLC (Method A-2): t_R = 13.7 min and 15.1 min; HPLC–MS (Method B): t_R = 12.1 min

and 12.9 min (2 tautomers); MS: (ESI^+), m/z (%): $[M + H]^+$ = 547.2 (100%); MS: (ESI^-), m/z (%): $[M - H]^-$ = 545.3 (100%), $[M - C_7H_7O - H]^-$ = 438.2 (30%); HRMS (ESI^-) calcd for $[C_{30}H_{30}N_2O_8 - H]^-$: 545.1929; found: 545.1956; λ_{abs}^{max} = 455 nm, λ_{em}^{max} = 516 nm, ε (λmax) = 5140 $M^{-1}cm^{-1}$, Φ = 0.243.

*N^6-((Benzyloxy)carbonyl-N^2-(2-(11-oxo-2,3,6,7-tetrahydro-1H,5H,11H-pyrano[2,3-f]pyrido[3,2,1-ij]quinolin-9-yl))acetyl)-L-lysine (**41**).* From compound **31** (0.150 g, 0.50 mmol, 1 eq), HCl.Lys(Cbz)-OMe (0.182 g, 0.55 mmol, 1.1 eq), HBTU (0.209 g, 0.55 mmol, 1.1 eq) and DIEA (346 µL, 2.0 mmol, 4 eq), compound **41** (0.033 g) was obtained by filtration, as a yellow powder in 12% yield, according to *General Procedure B*. ^{1}H NMR (500 MHz, CD_3OD): δ 7.40 (m, 5H, H-Ph) 7.15 (s, 1H, H-8), 6.01 (s, 1H, H-10), 5.06 (s, 2H, CH_2-Ph), 4.40 (m, 1H, H-α), 3.72 (s, 2H, CH_2–Coum), 3.27 (m, 4H, CH_2N), 2.84–2.71 (m, 6H, 2×CH_2-Ar, H-ε), 1.98-1.91 (m, 5H, 2 × CH_2-C*H*$_2$-CH_2, H-β), 1.75 (m, 1H, H-β), 1.62–1.41 (m, 4H, H-γ, H-δ); ^{13}C NMR (126 MHz, CD_3OD): δ 175.6 (CO_2H), 171.6 (CONH), 165.3, 161.4 (CO-Coum), 159.1 ($NHCO_2$), 152.7, 152.3, 147.7 (Cq-Ar), 138.3 (Cq-Ar), 129.6 (2×CH-Ar), 129.1(CH-Ar), 128.8 (3×CH-Ar), 123.3 (CH-Ar), 118.7 (Cq-Ar), 109.2 (CH-Ar), 108.8 (Cq-Ar), 67.5 (O*C*H$_2$-Ph), 51.0 (C-α), 50.5, 50.4 (CH_2-N), 41.5 (CH_2–Coum), 40.1 (C-ε), 32.0 (C-β), 30.8 (C-δ), 28.8 (CH_2), 24.1 (C-γ), 22.5, 21.6, 21.4 (CH_2); HPLC (Method A-2): t_R = 17.0 min; HPLC–MS (Method B): t_R = 15.0 min; MS: (ESI^-), m/z (%): $[M - H]^-$ = 560.5 (100%), $[M - C_7H_8O - H]^-$ = 452.4 (30%); HRMS: (ESI^-) calcd for $[C_{31}H_{35}N_3O_7 - H]^-$: 560.2402; found: 560.2424; λ_{abs}^{max} = 395 nm, λ_{em}^{max} = 487 nm, ε (λmax) = 8870 $M^{-1}cm^{-1}$, Φ = 0.736.

*N^6-((Benzyloxy)carbonyl-N^2-(((7-hydroxy-2-oxo-2H-chromen-4-yl)methoxy)carbonyl)-L-lysine (**42**).* 7-Hydroxy-4-hydroxy methyl-coumarin **27** (0.150 g, 0.78 mmol, 1eq) and CDI (0.156 g, 0.93 mmol, 1.2 eq) was added in dry DMF (2 mL) and the solution was stirred for 3 h at room

temperature leading to a white precipitate. HCl.Lys(Cbz)-OMe. (0.307 g, 0.93 mmol, 1.2 eq) and DIEA (215 µL, 1.25 mmol, 1.6 eq) were added in solution and heated to 80 °C for 1.5 h. After cooling to room temperature, the pH was adjusted to 3 with aqueous HCl (1 M) and solution was extracted with EtOAc (2×30 mL). Organic layer was washed with H_2O (2×20 mL), dried (Na_2SO_4), filtered and evaporated. After purification by column chromatography on silica gel (EtOAc), the ester compound was diluted with a solution of aqueous LiOH (0.5 M)/THF (3 mL, 1/1) and stirred at room temperature for 2 h. THF was removed under vacuum and the pH was adjusted to 2 with aqueous HCl solution (1 M), then extracted with EtOAc (2×15 mL). Organic layers were dried (Na_2SO_4), filtered and evaporated. The residue was purified by column chromatography on silica gel (CH_2Cl_2/MeOH/AcOH: 85/15/1). Compound **42** (0.080 g) was obtained as a white gum in 21% yield. Mp 72–73 °C; ^{1}H NMR (500 MHz, CD_3OD): δ 7.44 (d, J = 9.0 Hz, 1H, H-5), 7.28 (m, 5H, H-Ph), 6.76 (dd, J = 8.5 Hz, J = 2.5 Hz, 1H, H-6), 6.68 (d, J = 2.5 Hz, 1H, H-8), 6.24 (s, 1H, H-3), 5.25 (s, 2H, CH_2-Ph), 5.02 (s, 2H, CH_2–Coum), 4.18 (m, 1H, H-α), 3.11 (t, J = 6.5 Hz, 2H, H-ε), 1.87,1.72 (2m, 2H, H-β), 1.54–1.42 (m, 4H, H-γ, H-δ); ^{13}C NMR (126 MHz, CD_3OD): δ 175.3 (CO_2H), 163.5, 163.0, 158.9 (Cq-O) 157.7 (Cq-Ar), 156.7 ($NHCO_2$), 153.2, 138.4 (Cq-Ar), 129.5 (2×CH-Ar), 128.9 (CH-Ar), 128.7 (2×CH-Ar), 126.4 (CH-Ar), 114.6 (CH-Ar), 111.0 (Cq-Ar), 108.9 (CH-Ar), 103.9 (CH-Ar), 67.4 (OCH_2-Ph), 62.0 (CH_2–Coum), 52.9 (C-α), 41.6 (C-ε), 32.4 (C-β), 30.4 (C-δ), 24.1 (C-γ); HPLC (Method A-2): t_R = 13.9 min; HPLC–MS (Method B): t_R = 12.9 min; MS: (ESI$^+$), m/z (%): $[M + H]^+$ = 499.1 (50%); $[2M + Na]^+$ = 1019.0 (100%); MS: (ESI$^-$), m/z (%): $[M - H]^-$ = 497.2 (100%); HRMS (ESI$^-$) calcd for $[C_{25}H_{26}N_2O_9 - H]^-$: 497.1565; found: 497.1567; λ_{abs}^{max} = 324 nm, λ_{em}^{max} = 395 nm, ε (λmax) = 11200 $M^{-1}cm^{-1}$, Φ = 0.12.

*N^2-(((9H-Fluoren-9-yl)methoxy)carbonyl)-N^6-(2-(7-(dimethylamino)-2-oxo-2H-chromen-4-yl)acetyl)-L-lysine (**44**).* From 7-Dimethylamino-4-carboxymethyl-coumarin **29** (0.247 g, 1.0 mmol, 1 eq), Fmoc-Lys-OMe **43** (0.442 g, 1.0 mmol, 1 eq), HBTU (416 mg, 1.1 mmol, 1.1 eq) and DIEA (865 µL, 5.0 mmol, 5 eq), compound **44** (0.030 g) was obtained, after purification by column chromatography on silica gel (CH_2Cl_2/MeOH/AcOH: 85/15/1), as a yellow powder in 5% yield, according to *General Procedure B*. ^{1}H NMR (500 MHz, CD_3OD): δ 7.76 (d, J = 7.5 Hz, 2H, H-Ar), 7.64 (d, J = 7.5 Hz, 2H, H-Ar), 7.51 (d, J = 9.0 Hz, 1H, H-5), 7.36 (t, J = 7.5 Hz, 2H, H-Ar), 7.28 (t, J = 7.5 Hz, 2H, H-Ar), 6.71 (dd, J = 9.0 Hz, J = 2.5 Hz, 1H, H-6), 6.48 (d, J = 2.5 Hz, 1H, H-8), 6.02 (s, 1H, H-3), 4.33 (d, J = 6.0 Hz, 2H, OCH_2CH), 4.18 (t, J = 6.0 Hz, 1H, OCH$_2$CH), 4.09 (m, 1H, H-α), 3.64 (s, 2H, CH_2–Coum), 3.21 (t, J = 6.5 Hz, 2H, H-ε) 3.01 (m, 6H, N(CH_3)$_2$), 1.84, 1.68 (2m, 2H, H-β), 1.56-1.38 (m, 4H, H-γ, H-δ); ^{13}C NMR (126 MHz, CD_3OD): δ 177.4 (CO_2H), 167.5 (CONH), 160.7 (CO-Coum), 155.5, 155.3 (Cq-O, $NHCO_2$), 152.7 (Cq-Ar), 151.4 (Cq-N(Me)2), 143.8, 140.6 (2×Cq-Fmoc), 127.5, 127.0 (2×CH-Fmoc), 126.0 (CH-Ar), 125.2 (2×CH-Fmoc), 120.0 (2×CH-Fmoc), 109.3 (CH-Ar), 108.9 (CH-Ar), 108.2 (Cq-Ar), 97.4 (CH-Ar), 65.2 (OCH$_2$CH), 52.00 (C-α), 46.7 (OCH$_2$*C*H), 40.1 (C-ε), 40.0 (2xNCH$_3$), 38.7 (CH_2–Coum), 32.0 (C-β), 28.9 (C-δ), 22.7 (C-γ); HPLC (Method A-2): t_R = 17.7 min; HPLC–MS (Method B): t_R = 15.2 min; MS: (ESI+), m/z (%): $[M + H]^+$ = 598.4 (100%); MS: (ESI^-), m/z (%): $[M - H]^-$ = 596.3 (100%); HRMS (ESI^-) calcd for $[C_{34}H_{35}N_3O_7 - H]^-$: 596.24022, found: 596.24084; λ_{abs}^{max} = 373 nm, λ_{em}^{max} = 447 nm, ε (λmax) = 17600 $M^{-1}cm^{-1}$, Φ = 0.599.

*N-(((9H-Fluoren-9-yl)methoxy)carbonyl)-S-((7-hydroxy-2-oxo-2H-chromen-4-yl)methyl)-L-cysteine (**45**).* 4-Chloromethyl-7-hydroxy-coumarin **25** (0.316 g, 1.5 mmol, 1eq) and Fmoc-Cys-OH **16** (0.515 g, 1.5 mmol, 1 eq) were diluted in dry THF (7.5 mL), then DIEA (785 µL, 4.5 mmol, 3 eq) was added dropwise and the solution was stirred overnight at room

temperature. After evaporation, the residue was purified by column chromatography on silica gel (CH_2Cl_2/MeOH/AcOH: 85/15/1). Compound **45** (0.272 g) was obtained as a white powder in 35% yield. ^{1}H NMR (500 MHz, $(CD_3)_2SO$): δ 12.18 (brs, 1H, CO_2H), 11.01 (brs, 1H, OH), 7.88 (d, J = 7.5 Hz, 2H, H-Ar), 7.71 (d, J = 7.0 Hz, 2H, H-Ar), 7.66 (d, J = 8.5 Hz, 1H, H-5), 7.40 (brt, J = 7.5 Hz, 3H, H-Ar, NH), 7.31 (t, J = 7.5 Hz, 2H, H-Ar), 6.78 (dd, J = 8.5 Hz, J = 2.0 Hz, 1H, H-6), 6.71 (d, J = 2.0 Hz, 1H, H-8), 6.24 (s, 1H, H-3), 4.29-4.22 (m, 3H, OCH_2CH), 4.10 (m, 1H, H-α), 3.91, 3.88 (AB, 2H, CH_2–Coum), 2.96 (dd, J = 13.5 Hz, J = 4.0 Hz, 1H, H-β), 2.80 (dd, J = 13.5 Hz, J = 4.5 Hz, 1H, H-β); ^{13}C NMR (126 MHz, $(CD_3)_2SO$): δ 172.0 (CO_2H), 161.3 (Cq-7), 160.1 (CO-Coum), 155.8, 155.4 (Cq-8a, $NHCO_2$), 152.4 (Cq-4), 143.8 (2×Cq-Fmoc), 140.7 (2×Cq-Fmoc), 127.6, 127.0 (2×CH-Fmoc), 126.9 (CH-5), 125.2 (2×CH-Fmoc), 112.8 (CH-6), 110.3 (CH-3), 110.0 (Cq-4a), 102.3 (CH-8), 65.6 (OCH_2CH), 54.2 (C-α), 46.6 (OCH_2CH), 33.4 (C-β), 31.3 (CH_2–Coum); HPLC (Method A-1): t_R = 20.3 min; HPLC (Method A-2): t_R = 16.2 min; HPLC–MS (Method B): t_R = 16.6 min; HPLC–MS (Method C): t_R = 5.8 min; MS: (ESI^+), m/z (%): $[M + H]^+$ = 518.2 (100%); MS: (ESI^-), m/z (%): $[M – H]^-$ = 516.1 (100%); HRMS (ESI^-) calcd for $[C_{28}H_{23}NO_7S – H]^-$: 516.1122, found: 516.1126; λ_{abs}^{max} = 328 nm, λ_{em}^{max} = 399 nm, ε (λmax) = 5960 $M^{-1}cm^{-1}$, Φ = 0.0922.

*N-(((9H-Fluoren-9-yl)methoxy)carbonyl)-S-((7-methoxy-2-oxo-2H-chromen-4-yl)methyl)-L-cysteine (**46**).* 4-Chloromethyl-7-methoxy-coumarin 26 (0.224 g, 1.0 mmol, 1 eq) and Fmoc-Cys-OH **16** (0.343 g, 1.0 mmol, 1 eq) were diluted in dry DMF (8 mL), then Et_3N (278 µL, 2.0 mmol, 2 eq) was added dropwise and the solution was stirred overnight at room temperature. After evaporation, the residue was purified by column chromatography on silica gel (CH_2Cl_2/MeOH/AcOH: 85/15/1). Compound **46** (0.152 g) was obtained as a white powder in 28% yield. ^{1}H NMR (500 MHz, $(CD_3)_2SO$): δ 7.88 (d, J = 7.5 Hz, 2H, H-Ar), 7.75 (d, J = 8.0 Hz, 1H,

H-Ar), 7.75 (d, *J* = 8.0 Hz, 1H, H-Ar), 7.70 (m, 2H, H-Ar), 7.40 (t, *J* = 7.5 Hz, 2H, H-Ar), 7.30 (t, *J* = 7.5 Hz, 3H, H-Ar, NH), 6.96 (s, 1H, H-Ar), 6.89 (d, *J* = 8.0 Hz, 1H, H-Ar), 6.32 (s, 1H, H-3), 4.33-4.17 (m, 3H, OCH_2CH), 4.05 (m, 1H, NHC*H*), 3.92 (m, 2H, CH_2–Coum), 3.82 (s, 3H, CH_3), 2.98 (dd, *J* = 13.5 Hz, *J* = 3.0 Hz, 1H, H-β), 2.81 (dd, *J* = 12.5 Hz, *J* = 8.5 Hz, 1H, H-β); ^{13}C NMR (126 MHz, $(CD_3)_2SO$): *δ* 172.1 (CO_2H), 162.2 (C=O Coum), 159.9 (Cq-OMe), 155.6, 155.3 (Cq-O, $NHCO_2$), 152.3 (Cq-Ar), 143.8 (2×Cq-Ar), 140.6 (2×Cq-Ar), 127.5, 127.0 (4×CH-Ar), 126.7 (CH-Ar), 125.2, 120.0 (4×CH-Ar), 111.8 (CH-Ar), 111.3 (CH-Ar), 111.2 (Cq-Ar), 100.9 (CH-Ar), 65.6 (OCH_2CH), 55.8, 55.7 (C-α, OCH_3), 46.6 (OCH_2CH), 33.7 (C-β), 31.3 (CH_2–Coum); HPLC (Method A-2): t_R = 18.0 min; HPLC–MS (Method B): t_R = 18.0 min; HPLC–MS (Method C): t_R = 10.8; MS: (ESI^+), m/z (%): $[M + H]^+$ = 532.2 (100%); (ESI^-), m/z (%): $[M - H]^-$ = 530.2 (60%), $[2M - H]^-$ = 1061.3 (100%); HRMS (ESI^-) calcd for $[C_{29}H_{25}NO_7S - H]^-$: 530.1279, found: 530.1277; λ_{abs}^{max} = 324 nm, λ_{em}^{max} = 396 nm, ε (λmax) = 8570 $M^{-1}cm^{-1}$, Φ = 0.0428.

*N-(((9H-Fluoren-9-yl)methoxy)carbonyl)-S-((6-chloro-7-hydroxy-2-oxo-2H-chromen-4-yl)methyl)-L-cysteine (**47**).* 4-Chloromethyl-6-chloro-7-hydroxy-coumarin **28** (0.049 g, 0.2 mmol, 1 eq) and Fmoc-Cys-OH **16** (0.068 g, 0.2 mmol, 1 eq) were diluted in dry DMF (2 mL), then DIEA (108 µL, 0.6 mmol, 3 eq) was added dropwise and the solution was stirred overnight at room temperature. After evaporation, the residue was purified by column chromatography on silica gel (CH_2Cl_2/MeOH/AcOH: 90/10/1). Compound **47** (0.035 g) was obtained as a white powder in 32% yield. ^{1}H NMR (500 MHz, $(CD_3)_2SO$): *δ* 12.85 (brs, 1H, CO_2H), 11.38 (brs, 1H, OH-Ar), 7.88 (m, 2H, H-Ar), 7.75 (d, *J* = 8.0 Hz, 1H, NH), 7.71 (d, *J* = 7.5 Hz, 2H, H-Ar), 7.41 (t, *J* = 7.5 Hz, 2H, H-Ar), 7.31 (t, *J* = 7.5 Hz, 2H, H-Ar), 6.91 (s, 1H, H-Ar), 6.31 (s, 1H, H-3), 4.33-4.15 (m, 4H, OCH_2CH, H-α), 3.96 (m, 2H, CH_2–Coum), 2.95 (dd, *J* = 13.5 Hz, *J* = 4.0 Hz, 1H, H-β), 2.76 (dd,

J = 13.5 Hz, J = 10.0 Hz, 1H, H-β); ^{13}C NMR (126 MHz, $(CD_3)_2SO$): δ 172.0 (CO_2H), 159.6 (CO Coum), 156.2, 155.9, 155.8, 153.6, 151.4, 143.8, 143.7 (Cq-Ar), 140.7 (2×Cq-Ar), 127.5, 127.0 (2×CH-Ar), 126.4 (CH-Ar), 125.2, 125.1 (CH-Ar), 120.0 (2xCH-Ar), 116.7 (Cq-Ar), 111.6 (CH-Ar), 110.9 (Cq-Ar), 103.4 (CH-Ar), 65.7 (O*C*H_2CH), 53.6 (C-α), 46.6 (OCH_2CH), 32.7 (C-β), 31.2 (CH_2–Coum); HPLC (Method A-2): t_R = 16.8 min; HPLC–MS (Method B): t_R = 17.6 min; HPLC–MS (Method C): t_R = 8.9 min; MS: (ESI$^+$), m/z (%): $[M + H]^+$ = 552.1 (100%); MS: (ESI$^-$), m/z (%): $[M – H]^-$ = 550.1 (100%).

Modeling and Docking Computation. *Homology Modeling.* The human sequence of sialin was retrieved from the UniProt database[59] under the code Q9NRA2. The DgoT template structure 6E9N[51] was retrieved form the Protein Data Bank. Sequence alignment was carried out using CLUSTAL W[60] as implemented in Discovery Studio (Dassault Systèmes BIOVIA, Discovery Studio, 2019) and further refined manually. The model was generated using MODELER[61] and the best out of 100 models was selected according to the PDF Total Energy.

Molecular Docking. Flexible docking of **45** to the inward-facing model was carried out using GOLD.[53] A set of nine residues with flexible side-chains was used to define the binding site: F50; Y54; R57; F115; F116; Y119; F179; Y306; and Y335. The goldscore was used to keep the best 10 out of 100 poses. Then the pose that showed the best orientation according to the hypothesis made from the biological data was selected and further refined through molecular dynamic simulation.

Molecular Dynamics Simulations. The system with protein and ligand was prepared in the CHARMM-GUI web server[62] in order to generate a membrane around the protein and solvate with water and ions. A heterogeneous membrane was chosen, made of 90% of POPG and 10% of cholesterol, and a TIP3 water model with NaCl (0.15 M) counter ions were chosen for the

solvation. The system was typed with CHARMM36m forcefield and NAMD 2.13 was used. The system was equilibrated through six constrained simulations for a total of 690ps, by gradually diminishing the force constraints at each steps. Following constraints were applied (each value represent an equilibration step): protein backbone (10 / 5 / 2.5 / 1 / 0.5 / 0.1 kcal/mol); protein side-chains (5 / 2.5 / 1.25 / 0.5 / 0.25 / 0.05 kcal/mol); lipid heads (5 / 5 / 2 / 1 / 0.2 / 0 kcal/mol); dihedral bonds (500 / 200 / 100 / 100 / 50 / 0 kcal/mol). Then a production dynamics of 20 ns was carried out in NPT conditions at 303.15°K without any constraints.

Cell culture. HeLa and HEK293 cells were grown at 37 °C under 5% CO2 in glucose-rich, Glutamax-I-containing Dulbecco's modified Eagle medium (DMEM) supplemented with 10% fetal bovine serum (FBS), 100U/ml penicillin and 100 µg/ml streptomycin.

Fibroblasts from Salla patients were obtained from the Finnish Institute for Health and Welfare (THL), Helsinki, Finland, and used in this study with ethical permission no 78/13/03/00/16 (22 March 2016), issued by the Ethics Committee of the Helsinki and Uusimaa Hospital District, Finland. The fibroblasts tested for sialic acid storage rescue carried compound heterozygote mutations in the *SLC17A5* gene: 115c→t/1007-1008del, corresponding to p.Arg39Cys/p.Leu336Trpfs at the protein level. Fibroblasts were grown at 37 °C under 5% CO_2 in glucose-rich, Glutamax-I-containing DMEM supplemented with 20% FBS, 100U/ml penicillin and 100 µg/ml streptomycin.

Expression of recombinant sialin. HeLa cells were transfected either by electroporation or lipofection. For electroporation, 2×106 HeLa cells in 50 µl ice-cold phosphate-buffer saline (PBS; pH 7.4) were mixed with 5 µg wild-type or R39C pEGFP-C2-sialin plasmid[6] and immediately subjected to 10 square pulses (200 V, 3 ms) delivered at 1 Hz by a GHT 1287 electropulsator (Jouan) with 4-mm-spaced electrodes. Cells were then diluted with 7 ml culture medium and

distributed into 14 wells from a 24-well culture plate containing glass coverslips. For lipofection, HeLa were plated (100 000 cells/well) into 24-well plates containing glass coverslips and transfected on the following day with Lipofectamine™ 2000 (Invitrogen) according to the manufacturer's protocol.

HEK 293 cells were plated (250 000 cells/well) into poly-D-lysine-coated 24-well plates and lipofected similarly with a construct carrying a sorting motif mutation[6] (pEGFP-C2-sialin L22G/L23G) to express human sialin at the plasma membrane.

Radiotracer flux assays. *N*-acetyl [6-^{3}H]neuraminic acid (20 Ci/mmol) and [4,5-^{3}H] Fmoc-L-Leucine (50 Ci/mmol) were purchased from American Radiolabeled Chemicals. L-[1,2,1',2'-^{14}C]-cystine (200 mCi/mmol) and L-[2,3,4,5-^{3}H]-proline (75 Ci/mmol) were from Perkin Elmer. [^{3}H]Neu5Ac uptake into whole HEK293 cells was measured 2 days after transfection as described[6] with minor changes. Cells were briefly washed and incubated for 15 min at room temperature with [^{3}H]Neu5Ac (12.5 nM; 0.05 µCi/well) in a medium buffered with MES-Na^{+} pH 5.0. After 2 brief ice-cold washes, the cellular radioactivity in the cells was counted by liquid scintillation with a Tri-Carb 4910TR counter (PerkinElmer). For classical experiments, inhibitors were added simultaneously with [^{3}H]Neu5Ac. However, for some experiments (Figure 6), inhibitors were pre-incubated for 15 min at pH 5.0, followed by 15- or 30-min washes in a medium buffered at pH 7.0 with MOPS-Na^{+} before measuring [^{3}H]Neu5Ac transport. For saturation kinetics, incubation was shortened to 10 min to keep measurements within the linear phase of uptake at all [^{3}H]Neu5Ac concentrations.

[^{3}H]-Fmoc-Leu-OH uptake was measured similarly using 2 µM (one tenth of IC_{50}) and 0.05 µCi/well of the tracer. To compare Fmoc-Leu-OH and Neu5Ac in Figure S1, [^{3}H]Neu5Ac transport was measured at a similar transporter occupancy (100 µM; 0.05 µCi/well).

Human cystinosin and rat LYAAT1 were assayed at the plasma membrane of HEK293 cells in MES-Na^+ pH 5.0 buffer one day after lipofection using [^{14}C]cystine (20 μM; 0.08 μCi/well) and [^{3}H]proline (100 μM; 0.1 μCi/well) as substrates, respectively, as previously described.[46,47]

Immunofluorescence analysis. Sialin distribution was analyzed 2 days after transfection as described.[6] Cells were fixed with 4% paraformaldehyde. After quenching with 50 mM NH4Cl and several washes, cells were permeabilized and blocked with 0.05% saponin and 0.2% BSA in PBS buffer containing Ca^{2+} and Mg^{2+}. Coverslips were then incubated for ≥1 h with mouse anti-LAMP1 antibodies (H4A3; Developmental Studies Hybridoma Bank) at 0.75 μg/ml in blocking buffer, washed and incubated with Cy3-conjugated donkey anti-mouse antibodies (Jackson ImmunoResearch) at 1.4 μg/ml in the same buffer. Coverslips were then washed and mounted on glass slides with Fluoromount-G (SouternBiotech). Epifluorescence micrographs were acquired under a 100× objective lens with a Nikon Eclipse TE-2000 microscope equipped with a CCD camera (Coolsnap). The intracellular distribution of recombinant sialin was classified into 3 categories (see Figure 8B) by an independent observer in a blind manner. In other experiments, sialin/LAMP1 colocalization was quantitated by assessing the spatial correlation between pixel intensities of the green and red channels. Dual-color images were imported into the Fiji version (http://fiji.sc) of ImageJ[63] and the Substract Background and Coloc 2 plugins were used to calculate Pearson's correlation coefficients across 20 to 25 cells per condition. Statistical analysis was made using Kruskal-Wallis nonparametric one-way ANOVA with post hoc Dunn's test. To test the effect of **45** on sialin localization, the compound was added during the transfection step. The **45**-supplemented culture medium was replaced by a fresh one every day until 4 h before cell fixation.

Quantification of sialic acid levels in cells by mass spectrometry. Two confluent 75-cm^2 flasks of human fibroblasts were used for each measurement. Cells were cultured for 2 days in the

presence of 30 or 168 μM **45** in 0.3% DMSO, or with DMSO alone for control, at 37 °C under 5% CO2. The **45**-supplemented culture medium was replaced by a fresh one twice. After the 2 days, cells were detached by trypsinization, washed with ice-cold PBS and centrifuged. The resulting cell pellets were flash-frozen and kept at -20 °C until measurement.

Sialic acid measurements were done with some differences in two laboratories. In one protocol, pellets were submitted to osmolysis by addition of 100 μL ultrapure water (1 h, 4 °C) and subsequently sonicated (3×20 s with 10-s resting intervals). At this stage, protein concentration was determined for further normalization using Micro BCA Protein Assay Kit (ThermoFisher). After centrifugation (3000 rpm, 10 min, 4°C), 3 volumes of ice-cold EtOH were added to the supernatant and the mixture was kept overnight at –20 °C and centrifuged at 10,000 rpm for 10 min to precipitate glycoproteins. The new supernatant (containing free saccharides) was dried under nitrogen flow while the new pellet was pooled with the previous one to extract protein- and lipid-bound saccharides. All samples were subsequently treated with 100 μL of trifluoroacetic acid (TFA) 0.1 M, 2 h, 80 °C for selective release of bound sialic acids and dried overnight into a vacuum concentrator (Concentrator 5301, Eppendorf). Dried samples were incubated with 50 μL of the derivatization solution containing 1,2-diamino-4,5-methylenedioxybenzene dihydrochloride (DMB, 7 mM), 2-mercaptoethanol (1 M), $Na_2S_2O_4$ (18 mM), and TFA (20 mM) for 2 h, at 50 °C, in the dark. Samples were kept at -20 °C before analysis. Quantitative analyses were performed by micro-LC/ESI MRM-MS^3 in positive ion mode on an amazon speed ETD ion trap mass spectrompeter (Bruker Daltonics) equipped with a standard ESI source and controlled by Hystar software (ver. 3.2). The identification of MS^2 fragment ions was based on previous papers.[64,65] DMB-coupled sialic acids separation was achieved on Prominence LC-20AB micro LC system (Shimadzu). Samples were diluted 10-fold in formic acid (0.1 %) and dilutions were

applied (5 µL) to a Luna 3µm analytical column (C18, 100 Å, 150x1 mm, Phenomenex) with isocratic elution in acetonitrile/methanol/water (4:6:90, v/v/v) at 60 µL.min^{-1}. Multiple reaction monitoring (MRM) of MS^3 was used for DMB-coupled sialic acids quantification (ion spray voltage 4500 V, dry gas slow rate 8 L.min^{-1}). Absolute quantifications were calculated by comparing ion intensities to a standard curve established for DMB-coupled sialic acids (Neu5Ac, Neu5Gc, KDN). Results were normalized for total protein amount (nmol of sialic acids/mg of protein).

In another protocol, 250 µL of a 85 µmol/L solution of Neu5Ac 1,2,3-$^{13}C_3$ (internal standard, IS; Sigma-Aldrich, ref. 649694) was added to each fibroblast pellet. Samples were sonicated (3×10 s with 5-s resting intervals in ice) and assayed for protein concentration. For free sialic acid, 100 µL of this homogenate were mixed with 150 µL acetonitrile (ACN), homogenized and centrifuged. For total sialic acid, 100 µL homogenate were mixed with 200 µL sulphuric acid (63 mM) and incubated for 1 hour at 80 °C for hydrolysis. Samples were supplemented with 450 µL ACN, homogenized and centrifuged. The two supernatants (free and bound sialic acid) were quantitated by LC/MS^2 as described.[66] Transitions 308.1>86.9 (for Neu5Ac) and 311.1>89.9 (for IS) were monitored with a declustering potential of -50V and a collision energy of -16V. Peak integration was performed with the Analyst software (version 1.6.2, Applied Biosystems©; smoothing width: 3 points). Neu5Ac concentrations were calculated from the Neu5Ac area/IS area ratio and the calibration curve (linear through zero), and normalized to protein concentration.

ASSOCIATED CONTENT

Supporting information (PDF)

Molecular formula strings (SMILES) and associated data (Excel file)

Sialin homology model docked with **45** (PDB)

AUTHOR INFORMATION

Corresponding Authors

*I.M.C.: Université de Paris, Laboratoire de Chimie et Biochimie Pharmacologiques et Toxicologiques, CNRS UMR 8601, 45 rue des Saints-Pères, F-75006 Paris, France. E-mail : isabelle.mccort@parisdescartes.fr

*B.G.: Université de Paris, SPPIN - Saints-Pères Paris Institute for the Neurosciences, CNRS UMR 8003, 45 rue des Saints-Pères, F-75006 Paris, France. E-mail : bruno.gasnier@parisdescartes.fr. Web: https://www.sppin.fr/the-teams/team-4-membrane-dynamics/

*C.A.: same address, E-mail: christine.anne@parisdescartes.fr

Present Addresses

‡P.A.G.: Department of Chemistry, Simon Fraser University, Burnaby, British Columbia, V5A 1S6, Canada

Author Contributions

F.A., I.M.C., B.G. and C.A. designed the research; L.D., N.P., A.C., I.F., C.D., P.A.G., R.F., I.M.C. and C.A. conducted the experiments; all authors analyzed the data; F.A., I.M.C., B.G. and C.A. wrote the paper.

Funding Sources

This work was supported by: the Agence Nationale de la Recherche (grant #ANR-15-CE14-0001-02 to B.G.); the Association Nationale de la Recherche et de la Technologie (ANRT) and Dassault Systèmes BIOVIA (CIFRE PhD scholarship n° 2018/0027 to A.C.). the Ministère de l'Enseignement Supérieur, de la Recherche et de l'Innovation (PhD fellowship to P.A.G.); the Neuropôle Région Ile-de-France (PhD fellowship to L.D.); and the Science Ambassador Program from Dassault Systèmes BIOVIA (to A.C. and F.A.).

ACKNOWLEDGMENT

We thank Dr. Aija Kyttälä from the Finnish Institute for Health and Welfare (THL) for acquiring the ethical permissions in Finland and providing Salla fibroblasts for this study. C.B. thanks the glycoconjugate analysis facility PAGes (http:// plateforme-pages.univ-lille1.fr) and the FRABio research federation.

ABBREVIATIONS

Bz, Benzoyl; Bzl, Benzyl; Cbz, Benzyloxycarbonyl; t-Bu, *tert*-Butyl; Boc; *tert*-Butoxycarbonyl; CDI, 1,1'-Carbonyldimidazole; DIEA, Diethylamine; DMF, Dimethylformamide; Fmoc, Fluoren-9-ylmethoxycarbonyl; HBTU, 2-(1H-Benzotriazol-1-yl)-1,1,3,3-tetramethyluronium hexafluorophosphate; MOMCl, Methoxymethyl chloride; RT, room temperature; TFA, Trifluoroacetic acid; THF, Tetrahydrofuran; TMSCl, Trimethylsilyl chloride; Trt, Trityl.

REFERENCES

(1) Reimer, R. J. SLC17: A Functionally Diverse Family of Organic Anion Transporters. *Mol. Aspects Med.* **2013**, *34*, 350–359.

(2) Iharada, M.; Miyaji, T.; Fujimoto, T.; Hiasa, M.; Anzai, N.; Omote, H.; Moriyama, Y. Type 1 Sodium-Dependent Phosphate Transporter (SLC17A1 Protein) Is a Cl--Dependent Urate Exporter. *J. Biol. Chem.* **2010**, *285*, 26107–26113.

(3) Blakely, R. D.; Edwards, R. H. Vesicular and Plasma Membrane Transporters for Neurotransmitters. *Cold Spring Harb. Perspect. Biol.* **2012**, *4*, a005595.

(4) Sawada, K.; Echigo, N.; Juge, N.; Miyaji, T.; Otsuka, M.; Omote, H.; Yamamoto, A.; Moriyama, Y. Identification of a Vesicular Nucleotide Transporter. *Proc. Natl. Acad. Sci. U. S. A.* **2008**, *105*, 5683–5686.

(5) Verheijen, F. W.; Vermedicimbeek, E.; Aula, N.; Beerens, C. E. M. T. M. T.; Havelaar, A. C.; Joosse, M.; Peltonen, L.; Aula, P.; Galjaard, H.; Van Der Spek, P. J.; Mancini, G. M. S. A New Gene , Encoding an Anion Transporter , Is Mutated in Sialic Acid Storage Diseases. *Nat. Genet.* **1999**, *23*, 462–465.

(6) Morin, P.; Sagné, C.; Gasnier, B. Functional Characterization of Wild-Type and Mutant Human Sialin. *EMBO J.* **2004**, *23*, 4560–4570.

(7) Wreden, C. C.; Wlizla, M.; Reimer, R. J. Varied Mechanisms Underlie the Free Sialic Acid Storage Disorders. *J. Biol. Chem.* **2005**, *280*, 1408–1416.

(8) Qin, L.; Liu, X.; Sun, Q.; Fan, Z.; Xia, D.; Ding, G.; Ong, H. L.; Adams, D.; Gahl, W. A.; Zheng, C.; Qi, S.; Jin, L.; Zhang, C.; Gu, L.; He, J.; Deng, D.; Ambudkar, I. S.; Wang, S.

From the Cover: Sialin (SLC17A5) Functions as a Nitrate Transporter in the Plasma Membrane. *Proc. Natl. Acad. Sci.* **2012**, *109*, 13434–13439.

(9) Miyaji, T.; Echigo, N.; Hiasa, M.; Senoh, S.; Omote, H.; Moriyama, Y. Identification of a Vesicular Aspartate Transporter. *Proc. Natl. Acad. Sci. U. S. A.* **2008**, *105*, 11720–11724.

(10) Lodder-Gadaczek, J.; Gieselmann, V.; Eckhardt, M. Vesicular Uptake of *N* -Acetylaspartylglutamate Is Catalysed by Sialin (SLC17A5). *Biochem. J.* **2013**, *454*, 31–38.

(11) Bardor, M.; Nguyen, D. H.; Diaz, S.; Varki, A. Mechanism of Uptake and Incorporation of the Non-Human Sialic Acid N-Glycolylneuraminic Acid into Human Cells. *J. Biol. Chem.* **2005**, *280*, 4228–4237.

(12) Chou, H. H.; Takematsu, H.; Diaz, S.; Iber, J.; Nickerson, E.; Wright, K. L.; Muchmore, E. A.; Nelson, D. L.; Warren, S. T.; Varki, A. A Mutation in Human CMP-Sialic Acid Hydroxylase Occurred after the Homo-Pan Divergence. *Proc. Natl. Acad. Sci. U. S. A.* **1998**, *95*, 11751–11756.

(13) Dhar, C.; Sasmal, A.; Varki, A. From “Serum Sickness” to “Xenosialitis”: Past, Present, and Future Significance of the Non-Human Sialic Acid Neu5Gc. *Front. Immunol.* **2019**, *10*, 807.

(14) Kawanishi, K.; Dhar, C.; Do, R.; Varki, N.; Gordts, P. L. S. M.; Varki, A. Human Species-Specific Loss of CMP- N -Acetylneuraminic Acid Hydroxylase Enhances Atherosclerosis via Intrinsic and Extrinsic Mechanisms . *Proc. Natl. Acad. Sci.* **2019**, *116*, 16036–16045.

(15) Büll, C.; Heise, T.; Adema, G. J.; Boltje, T. J. Sialic Acid Mimetics to Target the Sialic Acid-Siglec Axis. *Trends Biochem. Sci.* **2016**, *41*, 519–531.

(16) Moons, S. J.; Adema, G. J.; Derks, M. T.; Boltje, T. J.; Büll, C. Sialic Acid Glycoengineering Using N-Acetylmannosamine and Sialic Acid Analogs. *Glycobiology* **2019**, *29*, 433–445.

(17) Aula, P.; Gahl, W. A. Disorders of Free Sialic Acid Storage. In *The Metabolic Molecular Basis of Inherited Disease, Eighth Edition*; Scriver, C. R., Beaudet, A. L., Sly, W. S., Valle, D., Childs, B., Kinzler, K. W., Vogelstein, B., Eds.; McGraw-Hill: New-York, 2001; pp 5109–5120.

(18) Aula, N.; Salomäki, P.; Timonen, R.; Verheijen, F.; Mancini, G.; Månsson, J.-E.; Aula, P.; Peltonen, L. The Spectrum of SLC17A5-Gene Mutations Resulting in Free Sialic Acid–Storage Diseases Indicates Some Genotype-Phenotype Correlation. *Am. J. Hum. Genet.* **2000**, *67*, 832–840.

(19) Renlund, M.; Tietze, F.; Gahl, W. A. Defective Sialic Acid Egress from Isolated Fibroblast Lysosomes of Patients with Salla Disease. *Science* **1986**, *232*, 759–762.

(20) Varho, T. T.; Alajoki, L. E.; Posti, K. M.; Korhonen, T. T.; Renlund, M. G.; Nyman, S. R. G.; Sillanpää, M. L.; Aula, P. P. Phenotypic Spectrum of Salla Disease, a Free Sialic Acid Storage Disorder. *Pediatr. Neurol.* **2002**, *26*, 267–273.

(21) Zielonka, M.; Garbade, S. F.; Kölker, S.; Hoffmann, G. F.; Ries, M. A Cross-Sectional Quantitative Analysis of the Natural History of Free Sialic Acid Storage Disease—an Ultra-Orphan Multisystemic Lysosomal Storage Disorder. *Genet. Med.* **2019**, *21*, 347–352.

(22) Sonninen, P.; Autti, T.; Varho, T.; Hämäläinen, M.; Raininko, R. Brain Involvement in Salla Disease. *Am. J. Neuroradiol.* **1999**, *20*, 433–443.

(23) Prolo, L. M.; Vogel, H.; Reimer, R. J. The Lysosomal Sialic Acid Transporter Sialin Is Required for Normal CNS Myelination. *J. Neurosci.* **2009**, *29*, 15355–15365.

(24) Stroobants, S.; Van Acker, N. G. G.; Verheijen, F. W.; Goris, I.; Daneels, G. F. T.; Schot, R.; Verbeek, E.; Knaapen, M. W. M.; De Bondt, A.; Göhlmann, H. W.; Crauwels, M. L. A.; Mancini, G. M. S.; Andries, L. J.; Moechars, D. W. E.; D'Hooge, R. Progressive Leukoencephalopathy Impairs Neurobehavioral Development in Sialin-Deficient Mice. *Exp. Neurol.* **2017**, *291*, 106–119.

(25) Morland, C.; Nordengen, K.; Larsson, M.; Prolo, L. M.; Farzampour, Z.; Reimer, R. J.; Gundersen, V. Vesicular Uptake and Exocytosis of L-Aspartate Is Independent of Sialin. *FASEB J.* **2013**, *27*, 1264–1274.

(26) Pitto, M.; Chigorno, V.; Renlund, M.; Tettamanti, G. Impairment of Ganglioside Metabolism in Cultured Fibroblasts from Salla Patients. *Clin. Chim. Acta.* **1996**, *247*, 143–157.

(27) Aula, N.; Jalanko, A.; Aula, P.; Peltonen, L. Unraveling the Molecular Pathogenesis of Free Sialic Acid Storage Disorders: Altered Targeting of Mutant Sialin. *Mol. Genet. Metab.* **2002**, *77*, 99–107.

(28) Biancheri, R.; Rossi, A.; Verbeek, H. A.; Schot, R.; Corsolini, F.; Assereto, S.; Mancini, G. M. S.; Verheijen, F. W.; Minetti, C.; Filocamo, M. Homozygosity for the p.K136E Mutation in the SLC17A5 Gene as Cause of an Italian Severe Salla Disease. *Neurogenetics* **2005**, *6*, 195–199.

(29) Thompson, C. M.; Davis, E.; Carrigan, C. N.; Cox, H. D.; Bridges, R. J.; Gerdes, J. M.

Inhibitor of the Glutamate Vesicular Transporter (VGLUT). *Curr. Med. Chem.* **2005**, *12*, 2041–2056.

(30) Pietrancosta, N.; Kessler, A.; Favre-Besse, F.-C.; Triballeau, N.; Quentin, T.; Giros, B.; El Mestikawy, S.; Acher, F. C. Rose Bengal Analogs and Vesicular Glutamate Transporters (VGLUTs). *Bioorg. Med. Chem.* **2010**, *18*, 6922–6933.

(31) Tamura, Y.; Ogita, K.; Ueda, T. A New VGLUT-Specific Potent Inhibitor: Pharmacophore of Brilliant Yellow. *Neurochem. Res.* **2014**, *39*, 117–128.

(32) Moriyama, Y.; Nomura, M. Clodronate: A Vesicular ATP Release Blocker. *Trends Pharmacol. Sci.* **2018**, *39*, 13–23.

(33) Pietrancosta, N.; Anne, C.; Prescher, H.; Ruivo, R.; Sagné, C.; Debacker, C.; Bertrand, H.-O.; Brossmer, R.; Acher, F.; Gasnier, B. Successful Prediction of Substrate-Binding Pocket in SLC17 Transporter Sialin. *J. Biol. Chem.* **2012**, *287*, 11489–11497.

(34) Huang, Y.; Lemieux, M. J.; Song, J.; Auer, M.; Wang, D. N. Structure and Mechanism of the Glycerol-3-Phosphate Transporter from Escherichia Coli. *Science.* **2003**, *301*, 616–620.

(35) Irwin, J. J.; Shoichet, B. K. ZINC - A Free Database of Commercially Available Compounds for Virtual Screening. *J. Chem. Inf. Model.* **2005**, *45*, 177–182.

(36) Jawalekar, A. M.; Meeuwenoord, N.; Cremers, J. G. O.; Overkleeft, H. S.; Van Der Marel, G. A.; Rutjes, F. P. J. T.; Van Delft, F. L. Conjugation of Nucleosides and Oligonucleotides by [3+2] Cycloaddition. *J. Org. Chem.* **2008**, *73*, 287–290.

(37) Lin, W.; Long, L.; Feng, J.; Wang, B.; Guo, C. Synthesis of Meso-Coumarin-Conjugated Porphyrins and Investigation of Their Luminescence Properties. *European J. Org. Chem.*

2007, *2007*, 4301–4304.

(38) Shibu, E. S.; Ono, K.; Sugino, S.; Nishioka, A.; Yasuda, A.; Shigeri, Y.; Wakida, S. I.; Sawada, M.; Biju, V. Photouncaging Nanoparticles for MRI and Fluorescence Imaging in Vitro and in Vivo. *ACS Nano* **2013**, *7*, 9851–9859.

(39) Wirtz, L.; Kazmaier, U. A Mild Titanium-Catalyzed Synthesis of Functionalized Amino Coumarins as Fluorescence Labels. *European J. Org. Chem.* **2011**, *2011*, 7062–7065.

(40) Kim, J. H.; Sumranjit, J.; Kang, H. J.; Chung, S. J. Discovery of Coumarin Derivatives as Fluorescence Acceptors for Intrinsic Fluorescence Resonance Energy Transfer of Proteins. *Mol. Biosyst.* **2014**, *10*, 30–33.

(41) Šebej, P.; Wintner, J.; Müller, P.; Slanina, T.; Al Anshori, J.; Antony, L. A. P.; Klán, P.; Wirz, J. Fluorescein Analogues as Photoremovable Protecting Groups Absorbing at ∼520 Nm. *J. Org. Chem.* **2013**, *78*, 1833–1843.

(42) Montalbetti, C. A. G. N.; Falque, V. Amide Bond Formation and Peptide Coupling. *Tetrahedron* **2005**, *61*, 10827–10852.

(43) Rudolf, K.; Eberlein, W.; Engel, W.; Pieper, H.; Entzeroth, M.; Hallermayer, G.; Doods, H. Development of Human Calcitonin Gene-Related Peptide (CGRP) Receptor Antagonists. 1. Potent and Selective Small Molecule CGRP Antagonists. 1-[N2-[3,5-Dibromo-N-[[4-(3,4-Dihydro-2(1H)-Oxoquinazolin-3-Yl)-1-Piperidinyl]Carbonyl]-D-Tyrosyl]-l-Lysyl]-4-(4-Pyr. *J.Med.Chem.* **2005**, *48*, 5921–5931.

(44) Mali, S. M.; Ganesh Kumar, M.; Katariya, M. M.; Gopi, H. N. HBTU Mediated 1-Hydroxybenzotriazole (HOBt) Conjugate Addition: Synthesis and Stereochemical Analysis

of β-Benzotriazole N-Oxide Substituted γ-Amino Acids and Hybrid Peptides. *Org. Biomol. Chem.* **2014**, *12*, 8462–8472.

(45) Vasko, R. C.; Rodriguez, R. A.; Cunningham, C. N.; Ardi, V. C.; Agard, D. A.; McAlpine, S. R. Mechanistic Studies of Sansalvamide A-Amide: An Allosteric Modulator of Hsp90. *ACS Med. Chem. Lett.* **2010**, *1*, 4–8.

(46) Sagné, C.; Agulhon, C.; Ravassard, P.; Darmon, M.; Hamon, M.; El Mestikawy, S.; Gasnier, B.; Giros, B. Identification and Characterization of a Lysosomal Transporter for Small Neutral Amino Acids. *Proc. Natl. Acad. Sci. U. S. A.* **2001**, *98*, 7206–7211.

(47) Kalatzis, V.; Cherqui, S.; Antignac, C.; Gasnier, B. Cystinosin, the Protein Defective in Cystinosis, Is a H+-Driven Lysosomal Cystine Transporter. *EMBO J.* **2001**, *20*, 5940–5949.

(48) Bizzarri, R.; Arcangeli, C.; Arosio, D.; Ricci, F.; Faraci, P.; Cardarelli, F.; Beltram, F. Development of a Novel GFP-Based Ratiometric Excitation and Emission PH Indicator for Intracellular Studies. *Biophys. J.* **2006**, *90*, 3300–3314.

(49) Yan, N. Structural Biology of the Major Facilitator Superfamily Transporters. *Annu. Rev. Biophys.* **2015**, *44*, 257–283.

(50) Drew, D.; Boudker, O. Shared Molecular Mechanisms of Membrane Transporters. *Annu. Rev. Biochem.* **2016**, *85*, 543–572.

(51) Leano, J. B.; Batarni, S.; Eriksen, J.; Juge, N.; Pak, J. E.; Kimura-Someya, T.; Robles-Colmenares, Y.; Moriyama, Y.; Stroud, R. M.; Edwards, R. H. Structures Suggest a Mechanism for Energy Coupling by a Family of Organic Anion Transporters. *PLoS Biol.* **2019**, *17*, 1–25.

(52) Mancini, G. M. S.; Beerens, C. E. M. T.; Aula, P. P.; Verheijen, F. W. Sialic Acid Storage Diseases: A Multiple Lysosomal Transport Defect for Acidic Monosaccharides. *J. Clin. Invest.* **1991**, *87*, 1329–1335.

(53) Jones, G.; Willett, P.; Glen, R. C.; Leach, A. R.; Taylor, R. Development and Validation of a Genetic Algorithm for Flexible Docking. *J. Mol. Biol.* **1997**, *267*, 727–748.

(54) Kleta, R.; Aughton, D. J.; Rivkin, M. J.; Huizing, M.; Strovel, E.; Anikster, Y.; Orvisky, E.; Natowicz, M.; Krasnewich, D.; Gahl, W. A. Biochemical and Molecular Analyses of Infantile Free Sialic Acid Storage Disease in North American Children. *Am. J. Med. Genet.* **2003**, *120A*, 28–33.

(55) Robichaud, T.; Appleyard, A. N.; Herbert, R. B.; Henderson, P. J. F.; Carruthers, A. Determinants of Ligand Binding Affinity and Cooperativity at the GLUT1 Endofacial Site. *Biochemistry* **2011**, *50*, 3137–3148.

(56) Blat, Y. Non-Competitive Inhibition by Active Site Binders. *Chem. Biol. Drug Des.* **2010**, *75*, 535–540.

(57) Morello, J. P.; Bouvier, M.; Petäjä-Repo, U. E.; Bichet, D. G. Pharmacological Chaperones: A New Twist on Receptor Folding. *Trends Pharmacol. Sci.* **2000**, *21*, 466–469.

(58) Parenti, G.; Andria, G.; Valenzano, K. J. Pharmacological Chaperone Therapy: Preclinical Development, Clinical Translation, and Prospects for the Treatment of Lysosomal Storage Disorders. *Mol. Ther.* **2015**, *23*, 1138–1148.

(59) UniProt: A Worldwide Hub of Protein Knowledge. *Nucleic Acids Res.* **2019**, *47*, D506–D515.

(60) Thompson, J. D.; Higgins, D. G.; Gibson, T. J. CLUSTAL W: Improving the Sensitivity of Progressive Multiple Sequence Alignment through Sequence Weighting, Position-Specific Gap Penalties and Weight Matrix Choice. *Nucleic Acids Res.* **1994**, *22*, 4673–4680.

(61) Šali, A.; Blundell, T. L. Comparative Protein Modelling by Satisfaction of Spatial Restraints. *J. Mol. Biol.* **1993**, *234*, 779–815.

(62) Jo, S.; Kim, T.; Iyer, V. G.; Im, W. CHARMM-GUI: A Web-Based Graphical User Interface for CHARMM. *J. Comput. Chem.* **2008**, *29*, 1859–1865.

(63) Schindelin, J.; Arganda-Carreras, I.; Frise, E.; Kaynig, V.; Longair, M.; Pietzsch, T.; Preibisch, S.; Rueden, C.; Saalfeld, S.; Schmid, B.; Tinevez, J.-Y.; White, D. J.; Hartenstein, V.; Eliceiri, K. ; Tomancak, P. ; Cardona, A. Fiji: An Open-Source Platform for Biological-Image Analysis. *Nature Methods*. Nature Publishing Group July 28, 2012, pp 676–682.

(64) Baumann, A. M. T.; Bakkers, M. J. G.; Buettner, F. F. R.; Hartmann, M.; Grove, M.; Langereis, M. A.; De Groot, R. J.; Muhlenhoff, M. 9-O-Acetylation of Sialic Acids Is Catalysed by CASD1 via a Covalent Acetyl-Enzyme Intermediate. *Nat. Commun.* **2015**, *6*, 7673.

(65) Noel, M.; Gilormini, P.-A.; Cogez, V.; Yamakawa, N.; Vicogne, D.; Lion, C.; Biot, C.; Guérardel, Y.; Harduin-Lepers, A. Probing the CMP-Sialic Acid Donor Specificity of Two Human β-D-Galactoside Sialyltransferases (ST3Gal I and ST6Gal I) Selectively Acting on O- and N-Glycosylproteins. *ChemBioChem* **2017**, *18*, 1251–1259.

(66) Piraud, M.; Pettazzoni, M.; Menegaut, L.; Caillaud, C.; Nadjar, Y.; Vianey-Saban, C.; Froissart, R. Development of a New Tandem Mass Spectrometry Method for Urine and

Amniotic Fluid Screening of Oligosaccharidoses. *Rapid Commun. Mass Spectrom.* **2017**, *31*, 951–963.

TABLE OF CONTENTS GRAPHIC